

THE EFFECTS OF TURBULENCE STRUCTURES ON THE
AIR-SIDE PERFORMANCE OF COMPACT TUBE-FIN HEAT
EXCHANGERS

By

Colin Bidden Allison

A Thesis submitted in fulfilment of the requirements for the
Degree of Doctor of Philosophy

SCHOOL OF MECHANICAL ENGINEERING
UNIVERSITY OF ADELAIDE



June 2006

© Colin Bidden Allison

Chapter 7

Effect of Streamwise Vortex Structures

7.1 Introduction

The findings from the previous chapter tend to suggest that the generation of span wise vortices, through passive means, does not enhance the air side convection coefficient adequately within the confines of the tube-fin geometry. There was a trade off between strut thickness (and spacing), and leading edge quantity. Transverse vortices by definition proceed crossways to the strut or fin direction. The advantage of streamwise vortices is that although they contain large rotational energy, they also travel parallel to the fins, hence are less likely to be constrained by them. The work undertaken in this chapter involves investigating the effect on heat transfer by stream wise vortices generated by a turbulence generator, or half delta-winglets arranged in various flow-up and flow-down configurations as shown in Figure 7.1.1.

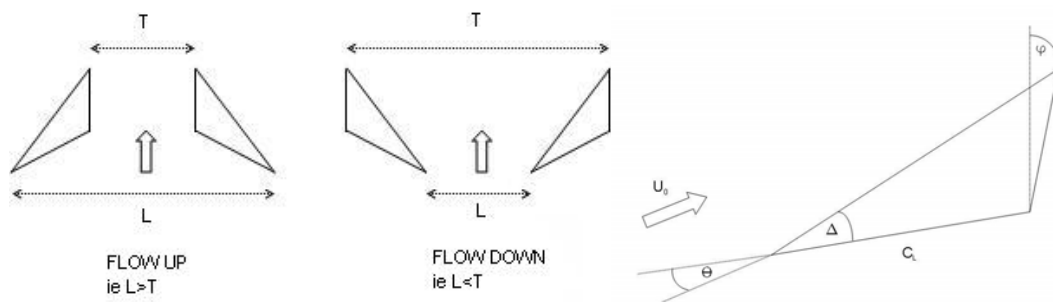


Figure 7.1.1 Sketch indicating the difference between flow-up and flow-down delta-winglet pairs, and the terminology associated with them

Apart from the vortex generation, the feasibility of incorporating additional leading edges along the fin surface would be sought. Initially a flow visualisation study was conducted to determine a vortex generator profile that would generate distinct stream

wise vortices. Then this profile was incorporated into a variety of fin designs combined with a tube bank, to determine suitable configurations for a full size coil prototype. The experimental assessment of the prototype was compared with previous results and those of the two louvre fin surfaces. Corresponding CFD modelling was undertaken to compare with experimental results hence validating the model. This model was then used to simulate the performance of various configurations and combinations of vortex generating arrangements in order to estimate the heat transfer potential of streamwise vortices in compact tube-fin geometry.

7.2 Design Philosophy

There have been numerous reports on heat exchanger performance with the delta winglets arranged in a flow-down configuration positioned directly in front of the tube, usually for the case of circular tubes[3, 9, 10]. However, it appears that any improvement in performance has not been conclusively described. A possible disadvantage of the flow-down design is that the orientation of the opposed winglets may cause a significant contribution of the bulk flow to be diverted around the tube, and therefore limit heat transfer due to flow impingement on the tubes which are the primary heat transfer surfaces.

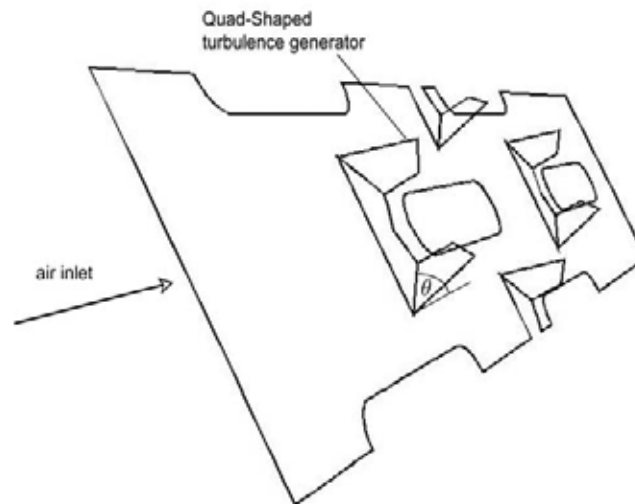


Figure 7.2.1 Sketch of the quad shaped turbulence generator arranged in a flow up configuration

To overcome this disadvantage, in this study the vortex generators were arranged in a flow-up configuration positioned directly in front of the tube, as shown in Figure 7.2.1. Also, instead of punching two separate vortex generators, it was decided to position the generators directly adjacent so that a common dividing line separated them. In this way, punching the generators out of the fin surface would leave a single opening with a broad edge facing the approaching flow. This exposed fin edge should theoretically restart the boundary layer along the fin surface, and this would occur in a location which is close to the tubes, thus combining each heat transfer mechanism at an elevated level. At this location there is a high temperature gradient between fin surface and bulk air flow on the one hand, and high Nusselt numbers due to boundary layer renewal on the other. Furthermore, it was thought that the flow-up configuration of the vortex generators would encourage the bulk flow to be guided onto the tube stagnation point, and the resulting high velocity gradients would increase the average Nusselt Number in this region as well. The actual generator shape that fitted these geometric requirements resulted in a quad shaped turbulence generator, rather than a triangular vortex generator.

In addition to the quad-shaped turbulence generator, several other configurations were trialled during the flow visualisation study. A typical delta winglet pair was arranged in a similar fashion to the aforementioned turbulence generators in a flow up configuration as shown in Figure 7.2.2.

Conversely a conventional flow-down configuration with delta-winglets was included in order to have a basis for comparison. Supposedly for these configurations the half-deltas would be separately punched from each other, so that the required delta profile could be achieved.

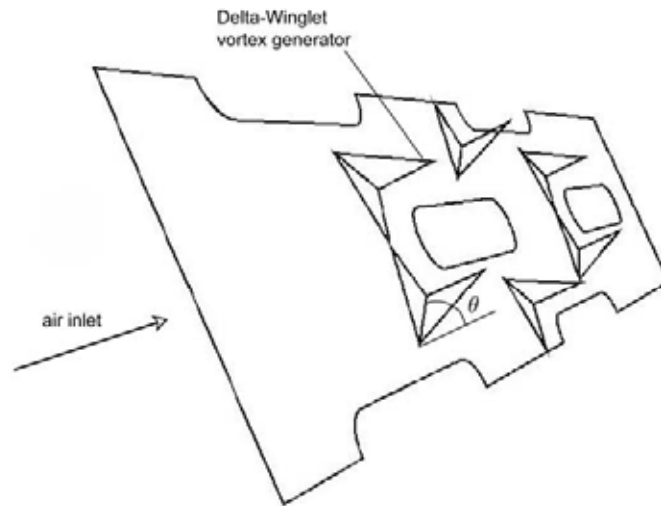


Figure 7.2.2 Sketch of the proposed delta winglet vortex generators arranged in the flow-up configuration

Finally, some flow visualisation was performed on models of plain fins having only the tube-hole flanges. This was done in order to establish any turbulence that may be generated at the tube fin junction, so that this could be distinguished from that generated by the various vortex generators.

7.3 Flow Visualisation Study

Although the profile of the quad-shaped turbulence generator was essentially fixed, it was necessary to establish a suitable delta profile. Preliminary qualitative evaluation of a variety of delta profile candidates at various angles of incidence produced a combination which demonstrated highly distinctive stream wise vortices. It was found that an angle of incidence Θ of 30 degrees combined with a delta angle Δ of 39 degrees produced coherent vortices with an acceptable longevity. An example of the vortices generated is shown in Figure 7.3.1.

Having optimised the winglet profile, models were fabricated for the visualisation consisting of various winglet configurations which were combined in pairs, as flow up and flow down orientations.

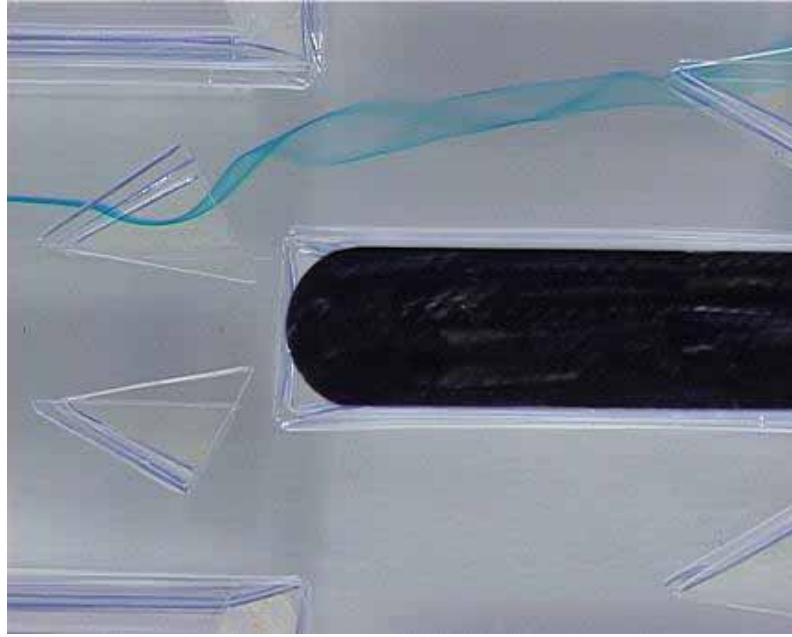


Figure 7.3.1 Vortex produced by a half delta winglet in the flow down configuration at a Reynolds Number of 4600

7.3.1 Model description

A perspex tube bundle was built as a basis upon which the different fins could be inserted at the required fin pitch. Several differences were necessary between this model and the previous range used for the parallel plate arrays which were described in Section 6.2.1. In order to model the thin copper fin, it was necessary to use a rigid yet thin plastic sheeting of 1.0mm thick. This meant scaling up the tube size by a factor of 6. Since the previous series of models were scaled up by a factor of 3 the current model is therefore twice the size of the previous model. This proved advantageous for the following reasons. Firstly the larger size meant that the tube bundle was able to encompass the complete depth of the water tunnel effectively eliminating the requirement to have flow control baffles for controlling the velocity profile in the vertical direction. Secondly for the same range of Reynolds Numbers to be tested, the flow speed in the tunnel could be halved. This greatly reduced the level of free stream turbulence levels of the approach flow. Since the method of introducing

the dye was using a hypodermic tube located upstream of the model the reduced turbulence levels reduced the possibility of unwanted turbulence shed from the probe.¹



Figure 7.3.2 Photograph of the dye release probe in proximity to the tube bundle located in the flow visualisation water tunnel

Figure 7.3.2 is a photograph showing a detail of the dye release probe in proximity to the tube bundle located in the water tunnel. For each fin vortex generating configuration, 3 identical fins were produced by cutting out the various delta wing profiles and bending them through 90 degrees. The acrylic that was used was chosen because it is semi-rigid and the vortex generators bent in this manner retained their shape. The tube holes and flanges were created by cutting a slit along the tube centre line and two diagonal slits radiating out from each end of the tube radius centre. The resulting flaps were also bent through 90 degrees. The resulting tube hole closely resembled the real tube hole that is created in the copper fin by the tube hole punching process. The 3 fins were slotted onto the centre of the tube bundle. The dye

¹ Recall that this problem was obviated in the previous perspex models by introducing the dye from within the tubes themselves and not from an upstream release point.

probe was positioned to release dye onto the leading vortex generator of the centre fin. The two outer fins were spaced at the scaled up fin pitch of 9fpi in order to create the appropriate boundary conditions.

The series of images in Figure 7.3.3 shows the range of the vortex generators used in the study.



a) Plain fin showing tube holes only



b) Turbulence generator



c) Flow Up Vortex generator



d) Flow Down Vortex generator

Figure 7.3.3 Photographs of the various Vortex generating devices

7.3.2 Procedure

Initially the plain fins were used to ensure that the upstream turbulence levels were acceptable for all flow velocities of interest. Also by studying the turbulence generated by the tube hole flanges clenching the tube, this turbulence could be isolated from that generated by the various vortex generators. This method of cutting flaps into the plastic sheeting for the tube hole flanges represented the most accurate method of simulating the turbulence generated from the tube and fin intersection. The dye probe had been mounted in a dial gauge stand so that the probe could be traversed

vertically. Each set of fin designs was tested at the three Reynolds Numbers corresponding to the air inlet velocities used for coil prototype performance evaluation. Recall that the Reynolds Numbers have been characterised by using the transverse tube pitch P_t as the length scale.

7.3.3 Results

The following series of images is a summary of selected frames captured from the video sequencing and summarises the results in a concise fashion. For each velocity a close-up image of the leading turbulence generator has been produced, as well as an elevation of the entire tube bundle in an attempt to capture the entire flow field through the tube bundle. These results are replicated at one of three vertical dye feed positions which releases dye on to the top and bottom of the vortex generator as well as the tube fin intersection. Due to dye dispersion with distance, the visualisation through the tube bundle was not as distinctive as desired.

Figure 7.3.5 through to Figure 7.3.9 show a selection of flow visualisation results for each type of fin surface. The dye release probe was traversed vertically with respect to each vortex generator. The positioning of the probe with respect to the geometry is explained in Figure 7.3.4.

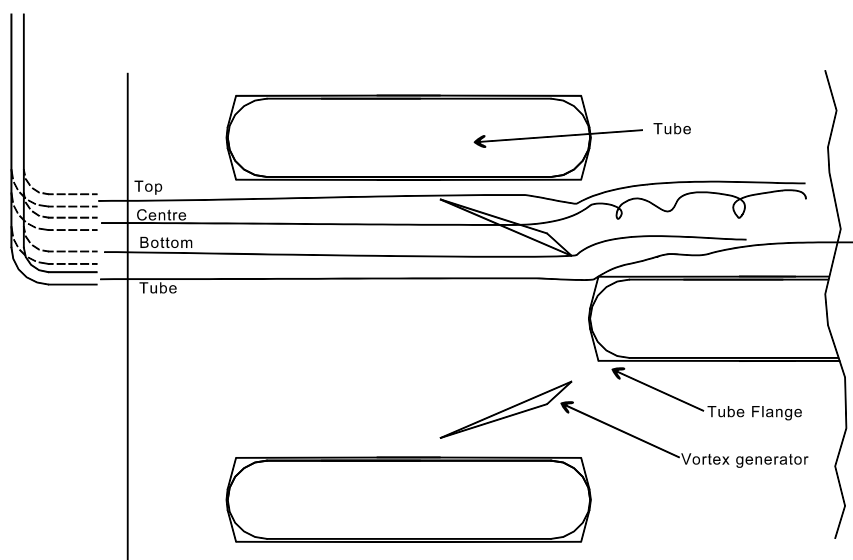


Figure 7.3.4 Sketch explaining the positioning of the dye release probe with respect to the vortex generator or tube

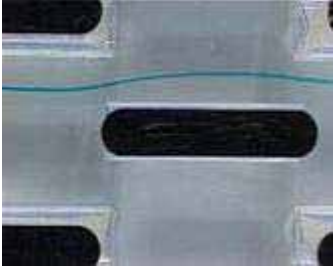



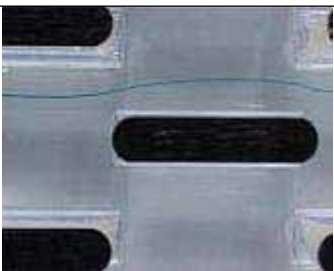







Dye Feed: Centre	Dye feed: Tube	u (m/s)
		2.9
		2.9
		4.8
		4.8
		6.3
		6.3

Figure 7.3.5 Plain fins at 9*phi*

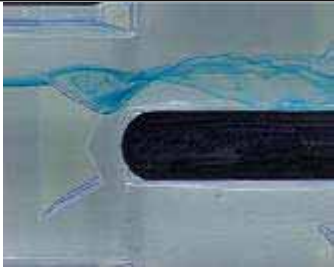
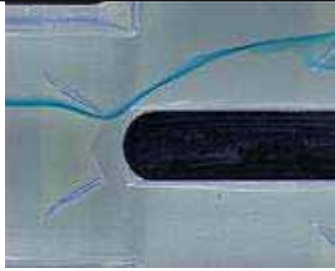
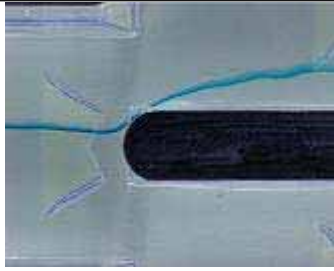

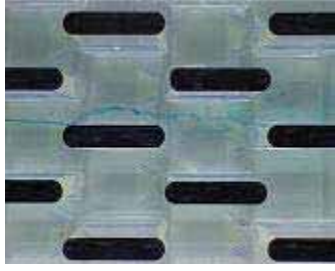

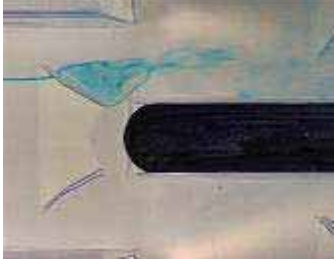
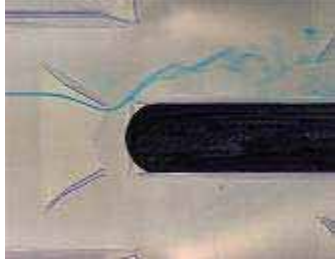
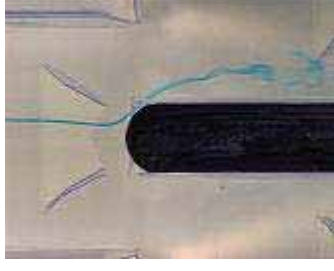



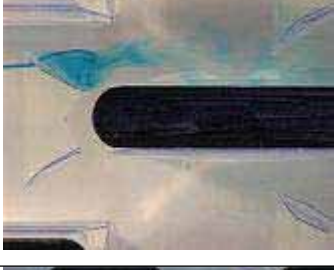





Dye Feed: Centre	Dye Feed: Bottom	Dye Feed: Tube	u (m/s)
			2.9
			2.9
			4.8
			4.8
			6.3
			6.3

Figure 7.3.6 Turbulence Generators at 9fpi

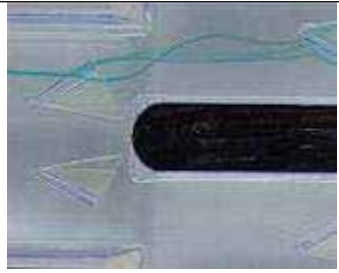

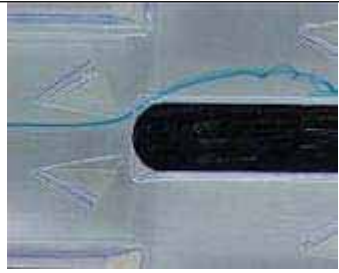
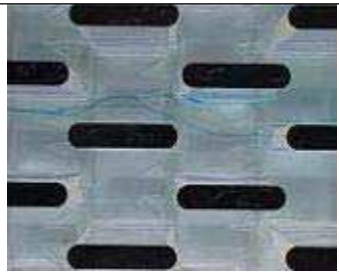
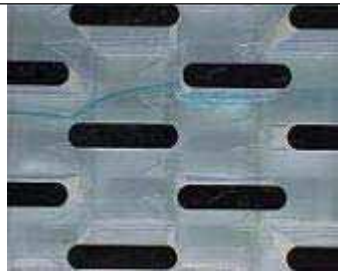
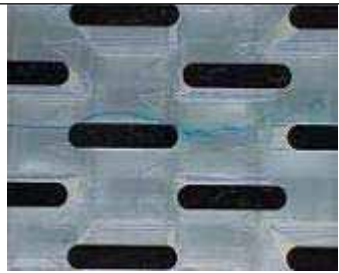






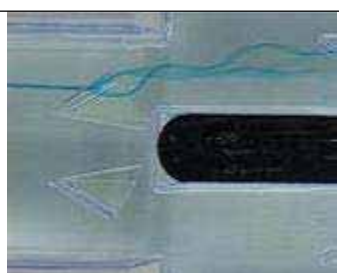

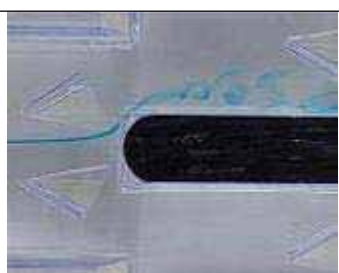



Dye Feed: Centre	Dye Feed: Bottom	Dye Feed: Tube	u (m/s)
			2.9
			2.9
			4.8
			4.8
			6.3
			6.3

Figure 7.3.7 Flow Down Vortex Generators at 9fpi



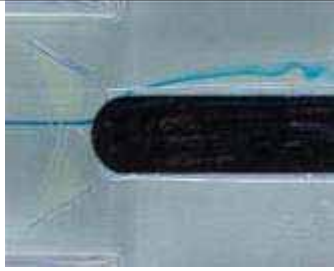





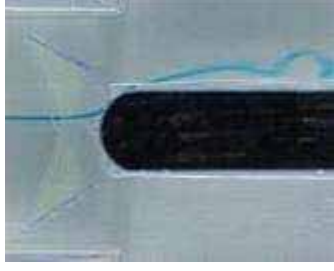









Dye Feed: Centre	Dye Feed: Bottom	Dye Feed: Tube	u (m/s)
			2.9
			2.9
			4.8
			4.8
			6.3
			6.3

Figure 7.3.8 Flow Up Vortex Generators at 9fpi

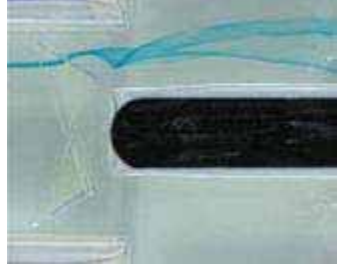

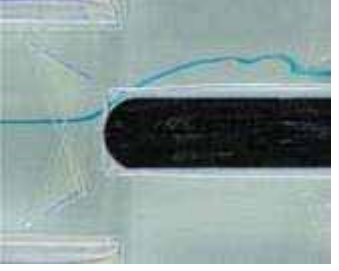
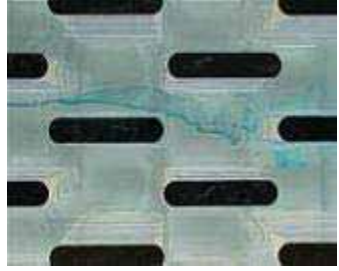
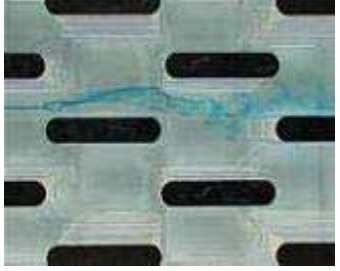

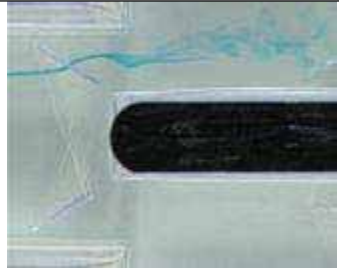
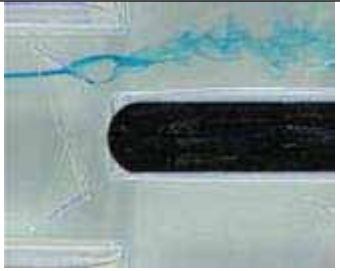
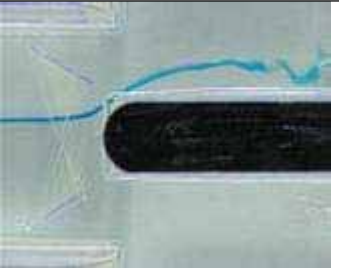



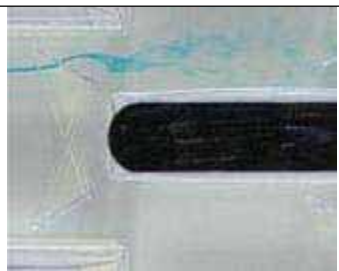

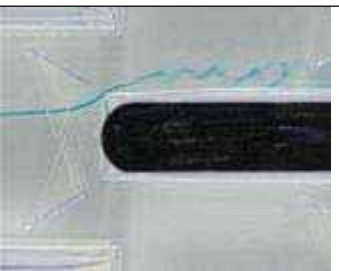



Dye Feed: Centre	Dye Feed: Bottom	Dye Feed: Tube	U (m/s)
			2.9
			2.9
			4.8
			4.8
			6.3
			6.3

Figure 7.3.9 Flow Up Vortex Generators at 4.5fpi

Observing Figure 7.3.5 it can be seen for the case of plane fins when the dye streak is released midway between the tubes that the flow appears steady and laminar through the tube bundle at each Reynolds number tested. As the dye streak is lowered onto the tube surface, there is some distinctive vortex shedding from the tube fin intersection.

From Figure 7.3.6 it can be seen that the turbulence generator creates a large separation area and stagnant fluid zone in its wake. This suggests that although turbulence levels may increase, an exceedingly high pressure drop may apply. Fluid approaching the tube along a centreline between the two opposing turbulence generators is seen to be diverted by the tube toward the adjacent tube rows. This occurs at all velocities, the turbulence levels increasing with Reynolds number. There are no coherent stream wise vortices generated and it appears that the turbulence levels are low in comparison to the high degree of separation produced. As a result of the flow visualisation, it was determined that although reasonable levels of turbulence were generated, the presence of coherent stream wise vortices did not occur. Also evident was a large separation area and stagnant fluid zone behind the turbulence generator.

Figure 7.3.7 shows distinct stream wise vortices generated from the flow down configuration. At low velocity, the vorticity is low compared to the free stream and it is swept down stream and transversely to intersect with the delta winglets in the adjacent row. As the velocity increases the vorticity level of the vortex increases but it is still swept downstream and transversely to intersect with the adjacent delta winglets at the same position. Although there are very distinctive vortices it is a concern that they are swept transversely as this may cause unnecessary interference when they impinge on the downstream delta winglets.

In Figure 7.3.8 the flow up configuration also shows distinctive stream wise vortices. In this case the vortex speed and hence vorticity level appears to be higher even though the vortex has a smaller diameter. Also the vortices are not deflected in the transverse direction and follow the free stream flow without impinging on the adjacent delta winglets. This configuration would appear to offer superior levels of vorticity and less

interference than the flow down configuration. In addition the fluid is channelled onto the tube stagnation point rather than being encouraged to flow around the tube.

The flow-up visualisation was also conducted at a fin spacing of 4.5fpi, in order to establish the effect of fin spacing. At this spacing the vortices are still generated but they are not as distinctive. They appear to diffuse into the free stream and decay into general turbulence after a short distance, although this phenomenon is to a lesser extent at the lowest speed. Hence it appears that the adjacent fin surfaces play a significant contributing factor in generating the vortices.

Based on the flow visualisation results, it was apparent that a pair of half-delta winglets arranged in a flow up configuration presented the most favourable characteristics that would contribute to improved heat transfer. The original philosophy of using quad-shaped turbulence generators did not facilitate the desired vortex generation. An additional consideration was the doubt that the quad-shaped turbulence generator could be practically achieved in a single punching process.

Based on the above considerations, it was decided not to proceed with the quad-shaped turbulence generator, apart from some Numerical simulations. For a working prototype coil, the flow-up delta winglet configuration was selected. A test coil having 9 fpi was fabricated and its performance assessed on the heat and mass flow test rig. These results were then directly compared with those of the two commercial louvre fin coils as discussed in Section 7.4 below.

7.4 Coil performance evaluation

Upon reviewing the flow visualisation results it was apparent that the delta-winglets arranged in a flow up configuration actually exhibited meaningful vortex generation. Therefore a working prototype based on the flow up configuration was fabricated and the performance assessed on the coil test rig.

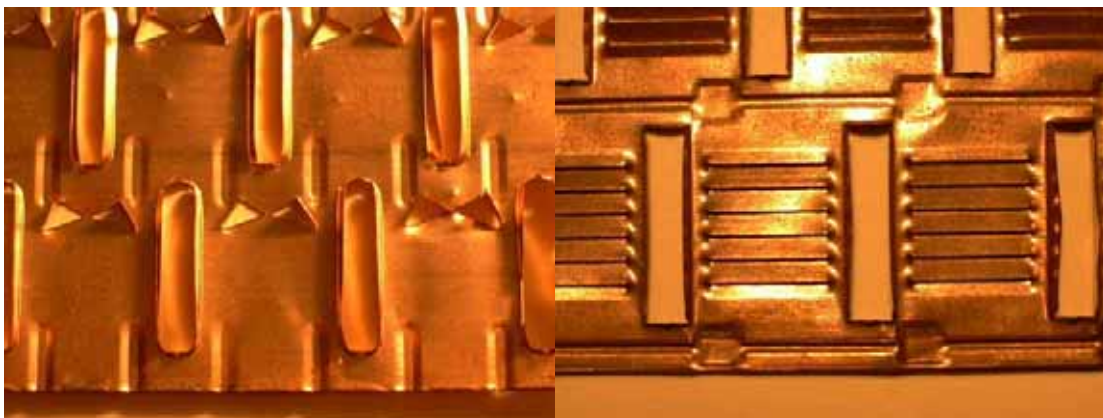
7.4.1 Coil description

A hand operated punch was fabricated which could locate and punch a pair of delta winglets at the designed orientation in front of each tube along the fin surface. This punch can be seen in the photograph in Figure 7.4.1.



Figure 7.4.1 Photograph of the hand operated punch designed to punch a delta winglet pair, and inset: a close up view of the punch and dye

The resulting copper fin surface with the array of delta winglets can be seen in Figure 7.4.2.a, and for comparison, the standard louvre surface is shown in Figure 7.4.2.b.



a) Delta Winglet surface

b) Louvre fin surface

Figure 7.4.2 Photographs of the Flow-Up delta winglet surface, and the louvre fin surface

The final quality of the punched winglets is excellent although because of the clearance between punch and dye, the winglet was not completely bent through 90 degrees after the punch was withdrawn. This resulted in the alignment of the winglets being between 15 and 20 degrees off the vertical, however this slight geometrical discrepancy is not expected to significantly affect the performance.

The coil that was fabricated had a fin pitch of 9 fins per inch and its performance was assessed on the coil test rig. A fin pitch of 9fpi was chosen for the prototype for the following reasons:

1. Since the design of the fin is to promote vortex generation it was considered counter productive to have a closer fin spacing which may reduce the effectiveness of the design.
2. The height of the deltas is 2.6mm and since the space between the fins of an 11fpi fin pitch is 2.3mm, the deltas would not be accommodated in this spacing.

7.4.2 Coil test results

The coil test results are presented in a series of performance comparison charts with the two louvre fin coils in Figure 7.4.3. They are also presented as a goodness factor comparison with the two louvre fin coils in Figure 7.4.4. In addition the Colburn j factor and friction fanning factor are presented graphically as a function of Reynolds number in Figure 7.4.5.

7.4.2.1 Performance Curves

As can be seen from Figure 7.4.3(a) the delta winglet fin design has a lower heat transfer capacity than the two standard louvre fin coils. Across the entire range of water flow rates, the capacity is approximately 78% and 87% of the 11fpi and 9fpi louvre fin coils respectively. Conversely the pressure drop of the DW coil is 44% and 54% of the 11fpi and 9fpi coils, respectively from Figure 7.4.3(b). This suggests that the vortex strength of the generated vortices and their location in proximity to the fin surface does not facilitate effective heat transfer. The lack of vortex strength is also attributable to the low pressure drop since generally the strength of a vortex is governed by the pressure drop across the vortex generator.

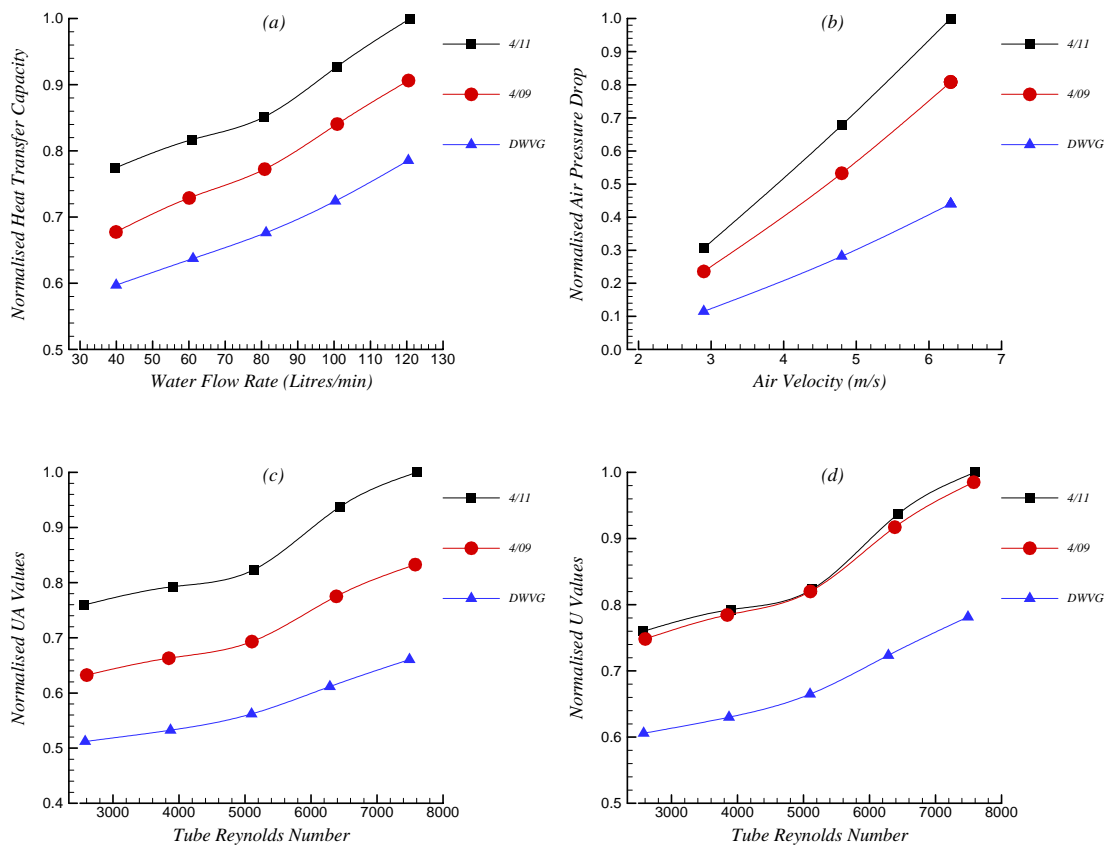


Figure 7.4.3 Performance comparison characteristics of the standard Lowvre fin surfaces versus the Delta Winglet vortex generator fin surface. Note that the results have been normalised with respect to the maximum values occurring for the 4/11 coil

The UA values in Figure 7.4.3(c) compare in a similar trend to that of the heat transfer capacity. Inspecting the U values in Figure 7.4.3(d) however indicates that the 9fpi coil has identical performance to the 11fpi coil. Although the capacity of the 9fpi is lower, it has a correspondingly lower heat transfer surface area. The DW coil has the same surface area as the 9fpi and this graph shows that the overall heat transfer coefficient of the DW coil is 78% of that of the two louvre coils.

7.4.2.2 Goodness Factor comparison

Figure 7.4.4 is a plot of a goodness factor comparison between the two commercial louvre fin coils and the Delta Wing coil.

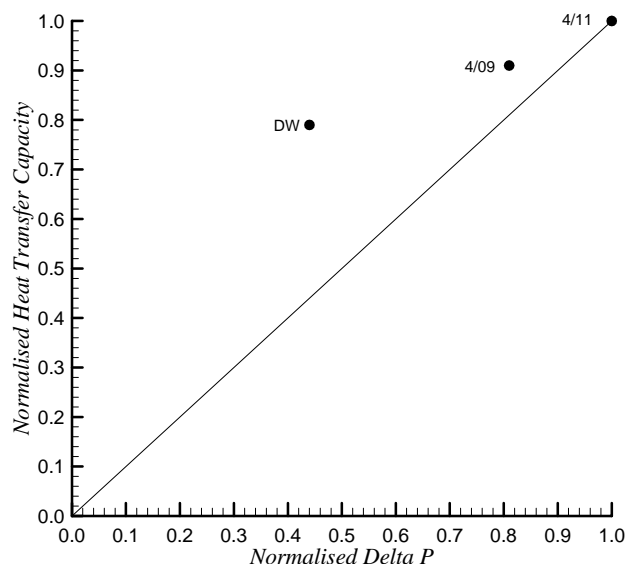


Figure 7.4.4 Experimental Goodness factor comparison of the two standard louvre fin coils and the Flow Up Delta Winglet coil

The DW coil has the best goodness factor and hence has the highest heat transfer capacity per unit pressure drop. However, the capacity of the DW coil is about 78% of the 4/11 coil and about 87% of the 4/09 coil. This implies that a 15% increase in coil area will achieve the same heat transfer but with almost half the pressure drop. There is then a direct saving in energy because the fan power consumption is the product of

flow rate and pressure drop. Although the air flow rate increases by 15%, the pressure reduces by 47%. The resulting power consumption $P_2 = 1.15 \times 0.47 P_1 = 0.54 P_1$.

The low pressure drop is encouraging and suggests the possibility of increasing the quantity of vortex generators, before the equivalent pressure drop of the standard coils may be exceeded. The contribution to heat transfer due to an increase in leading edges and that contributed from additional turbulence needs to be weighed up against a potential decrease in heat transfer due to excessive flow interference, separation and stagnation. Referring to previous findings in Chapter 6 on Parallel Plate arrays, that doubling or even tripling the quantity of struts and hence leading edges produced an increase in capacity but not in proportion to the increase in struts. So although it is suggested that increasing the number of vortex generators may actually increase the performance proportionally, this may not necessarily be the case. A Numerical simulation was performed to estimate the effect of increasing the quantity of vortex generators and the results are discussed in Section 7.4.2.4.

7.4.2.3 j -factor and f -factor comparison

In order to produce results for comparison purposes with other fin surfaces it is useful to publish this information in terms of the Colburn j factor and the friction fanning factor f . Figure 7.4.5 is a plot comparing the j and f factors of the two commercial louvre fin coils and the prototype Delta Winglet coil. Note that the Reynolds numbers plotted along the X-axis have been calculated based on the tube and fin cross sectional distance rather than the transverse tube pitch,

The j factor comparison shows that the heat transfer performance of the DW coil falls short of that of the two commercial coils by about 35%. Similarly the friction factor of the DW coil is lower than the standard coils by approximately 48%. These results agree with the previous observations of capacity and pressure drop.

It is clear that the heat transfer mechanisms of the two fin surfaces differ dramatically. The louvre fin surface facilitates boundary layer renewal and has numerous leading edges. The delta-winglet fin has fewer leading edges and relies predominantly on increasing convection through vortex generation. According to the results, the louvre

fin is superior to the Delta-winglet fin. Although coherent vortices were generated from the first row of winglets, it is doubtful whether the downstream winglets produce the same level of vorticity. This implies that only the first row of winglets may be effective in producing vortices which can improve heat transfer. In addition, the longevity of the vortices produced by the first row of winglets may be compromised by interference from the tubes and downstream winglets. Hence it is probable that only the fin surface area near to the first row of winglets experiences any major improvement in heat transfer coefficient. This finding necessitates the further exploration of ways to improve heat transfer at the downstream tube rows in order to fully utilise the potential of this type of fin.

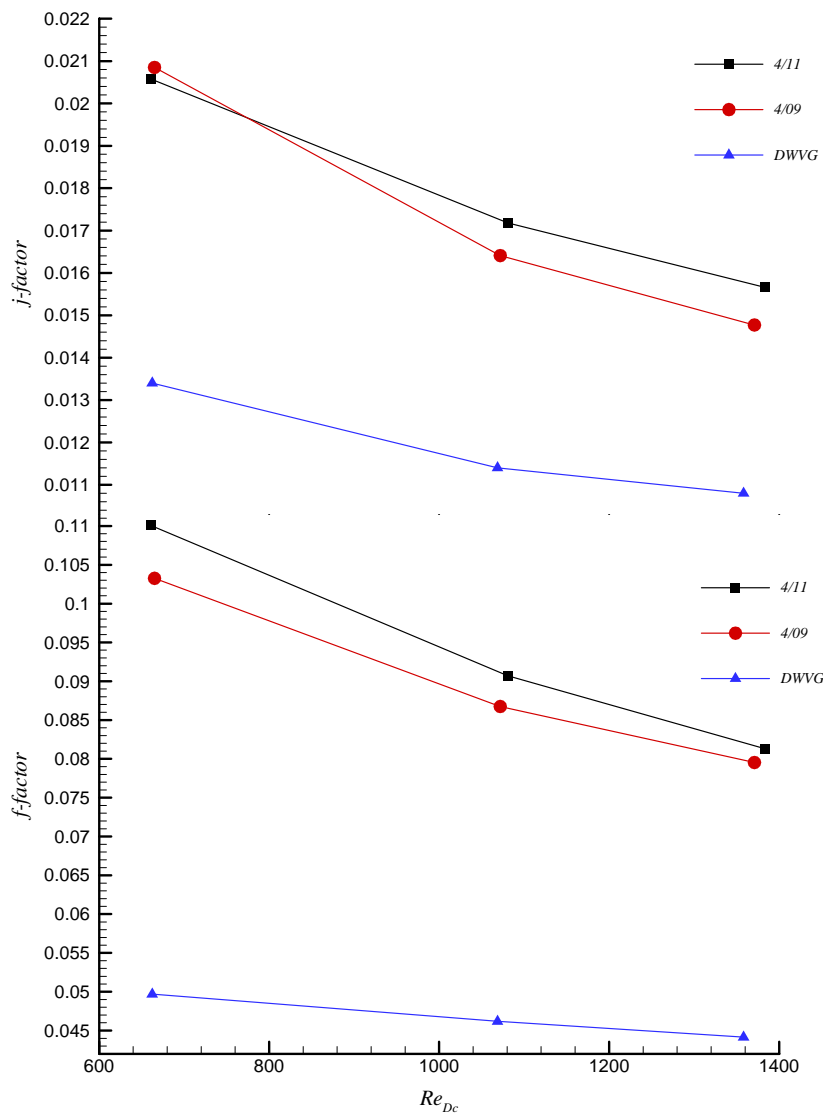


Figure 7.4.5 Comparison of j -factor and f -factor between the two louvre fin coils and the delta winglet prototype coil

7.4.2.4 Performance Assessment of Delta Winglet surface at elevated air velocities

The significantly lower pressure drop of the delta-winglet surface suggests that it can accommodate considerably higher air velocities before reaching the pressure drop of the louvre coils. It is possible that at an elevated air velocity, the increase in heat transfer may improve sufficiently to exceed that of the louvre fin coil at a comparable pressure drop. Alternatively a comparative heat transfer performance may be achievable at a lower pressure drop.

In order to investigate this possibility, the delta-winglet coil was experimentally assessed at an increased air velocity up to 8.2m/s. In Figure 7.4.6 the performance of the coil is compared with the louvre fin surface which also has 9 fins per inch.

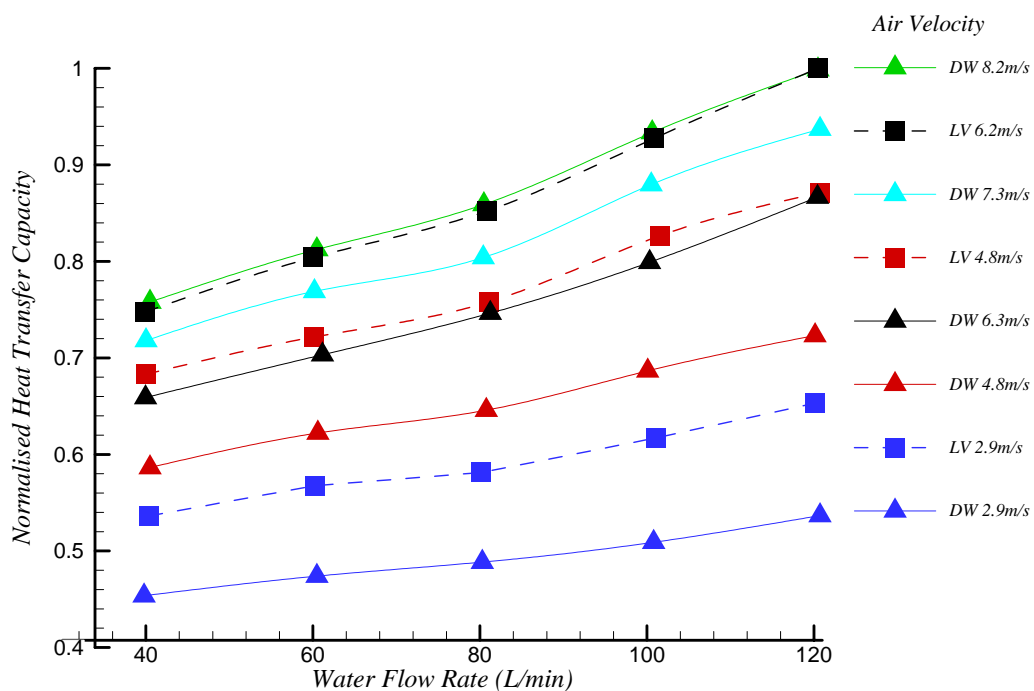


Figure 7.4.6 Heat transfer capacity comparison of the delta-winglet surface at elevated inlet air velocities, with the louvre fin surface having 9fpi.

It can be seen that at an air velocity of 8.2m/s the heat transfer capacity of the delta-winglet coil is equivalent to or marginally greater than that of the louvre fin surface at an air velocity of 6.3m/s. This improvement requires a 30% increase in air velocity.

Figure 7.4.7 is a plot comparing the air pressure drop of the louvre fin coil, and the delta-winglet coil inclusive of the elevated inlet air velocities. At the inlet velocity of 8.2m/s the air pressure drop of the delta-winglet coil is 89% of that of the louvre fin coil. Hence an equivalent heat transfer performance is achievable with the delta-winglet coil with only 89% air pressure drop at a 30% increase in inlet air velocity.

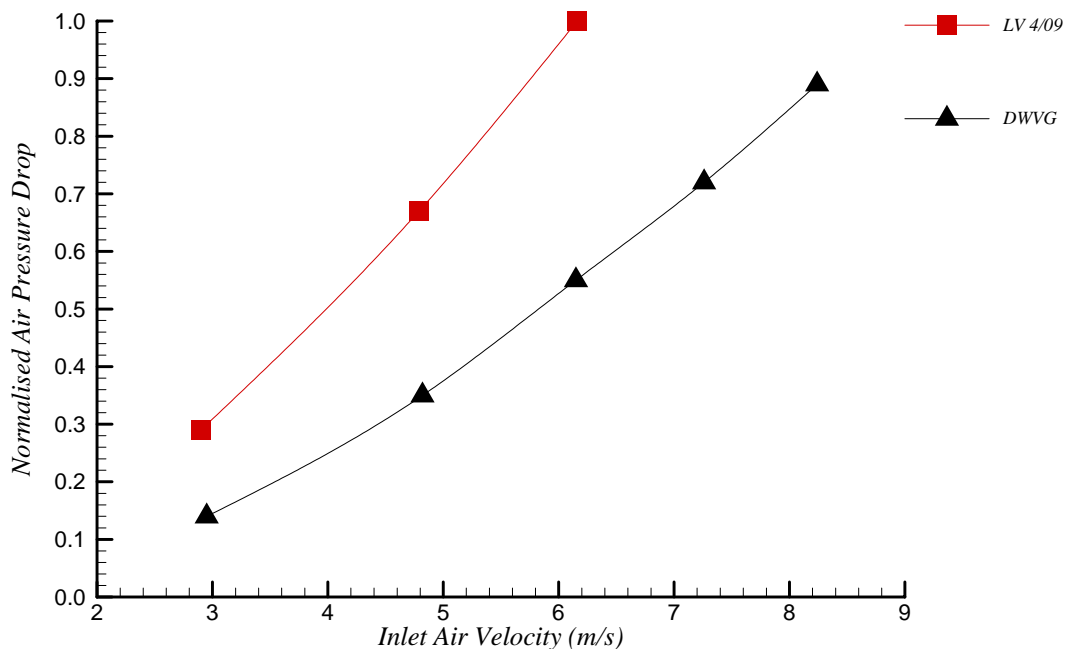


Figure 7.4.7 Heat transfer capacity comparison of the delta-winglet surface at elevated inlet air velocities, with the louvre fin surface having 9fpi.

7.5 CFD Study

Having assessed each coil performance, a CFD model of the delta-winglet fin surface was developed. The comparison between experimental coil results was then used to validate the corresponding CFD models. An excellent comparison between experimental prototypes and CFD models was obtained. Having established a high degree of confidence in the validity of the model, various geometrical variations could be simulated and the performance compared on a relative basis. A useful range of simulations were performed to establish the effect of a variation in the delta alignment from the vertical. It is typically assumed that the deltas form a normal angle with the fin surface. It is possible that a delta lean off the vertical may show a reduction in pressure drop. This aspect of the geometry has not been considered previously, and is therefore useful information. In addition a series of CFD models having a variety of combinations of multiple pairs of vortex generators arranged in various combined flow up and flow down configurations was undertaken.

7.5.1 Model geometry

The size of the computational domain was kept consistent with that of the louvre fin geometry described previously. The fin surface and protruding deltas were modelled as a thin surface allowing conjugate heat transfer. However a departure from the actual geometry is the omission of the tube-hole flanges which are not incorporated in the geometry. Figure 7.5.1 shows a sketch of the resulting mesh covering the fin surface. Note the refinement of the mesh in the region of the Delta Winglets.

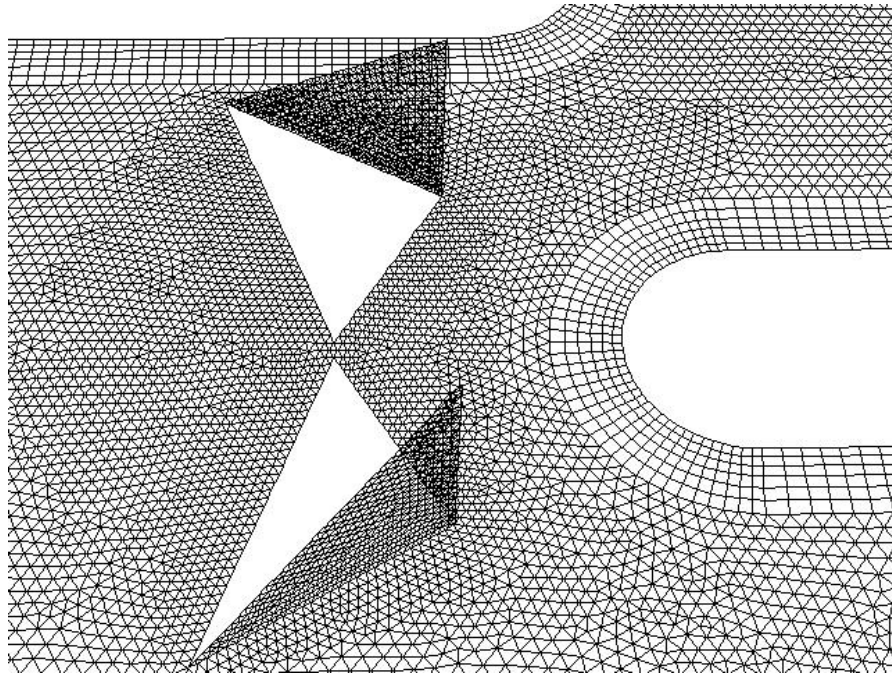


Figure 7.5.1 Sketch of the typical mesh covering the flow up delta winglet configuration

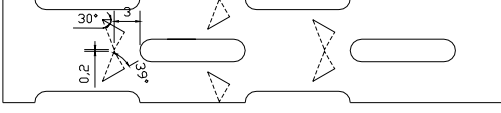

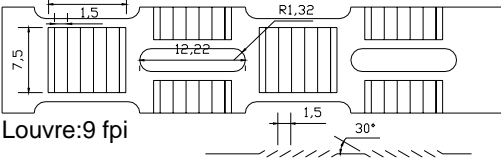

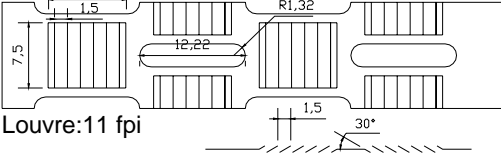
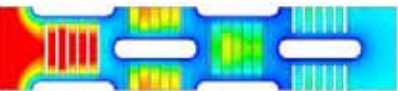
7.5.2 Modelling results

The results are presented as heat transfer capacity and pressure drop comparisons relative to the louvre fin surface having 11 fpi.

7.5.2.1 Model Validation

Initially, the simulation results of the delta winglet pair arranged in the flow up configuration was compared to the louvre fin simulations. Table 7.1 summarises these findings.

Table 7.1 Simulation comparison of performance of flow-up delta winglets with louvre fin surfaces

Fin Geometry	Fin temperature contours	\dot{Q}	ΔP
 <p>Delta Winglet Flow Up: x=-3mm</p>		0.75	0.66
 <p>Louvre:9 fpi</p>		0.92	0.85
 <p>Louvre:11 fpi</p>		1.00	1.00

Note that these results have been normalised and compared against normalised values of the experimental measurements, and are presented as goodness factors in the plot shown in Figure 7.5.2. It is evident that for each simulated heat transfer value a comparison with its experimental counterpart is in good agreement. With respect to pressure drop the comparison is not as accurate. The prediction of pressure drop in the case of the 9fpi is higher than the experimental measurement, and for the delta winglet surface this over prediction is even higher.

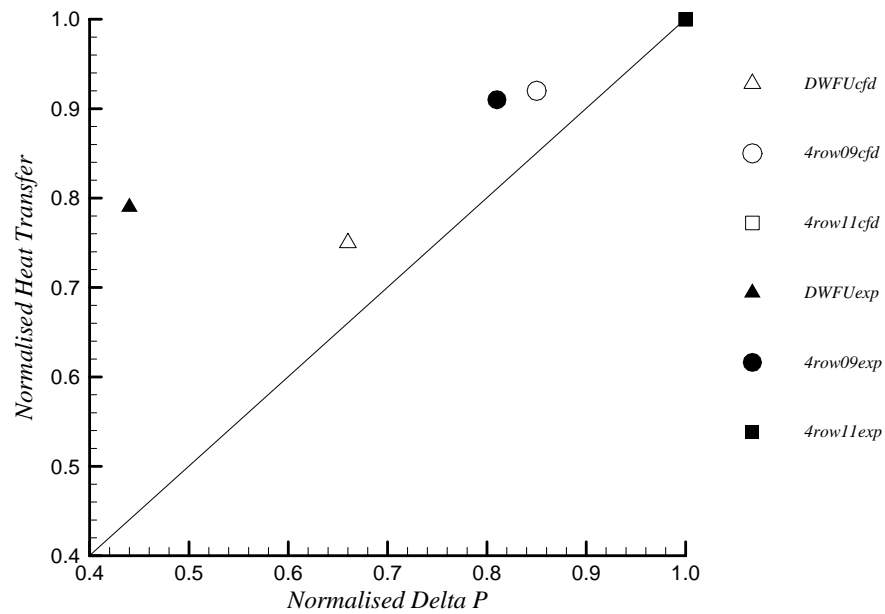
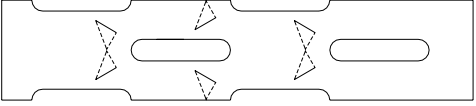

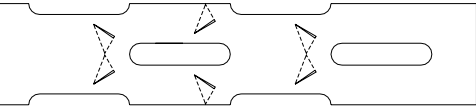

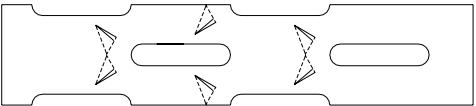



Figure 7.5.2 Simulated Numerical Goodness factor comparison of the Flow Up delta winglet and louvre fin surfaces, with the corresponding experimental results for CFD validation

A series of simulations were performed in order to investigate the effect of misalignment of the deltas by including an angle φ from the vertical position. It is thought that a delta wing which does not form a 90° angle with the fin may have a lower pressure drop. Table 7.2 summarises the results of the simulations obtained with delta winglets bent by an angle φ off the vertical position.

Table 7.2 Simulation comparison of Delta Winglet performance with varying altitude angle φ

Off Vertical Angle (φ)	Fin temperature contours	\dot{Q}	ΔP
 <p>Delta Winglet Flow Up: $\varphi=0^\circ$</p>		1.00	1.00
 <p>Delta Winglet Flow Up: $\varphi=10^\circ$</p>		0.99	0.95
 <p>Delta Winglet Flow Up: $\varphi=20^\circ$</p>		0.99	0.89

The results from Table 7.2 imply that the pressure drop does indeed reduce as the angle φ is increased. Interestingly the effect of φ on heat transfer is negligible. This is an interesting find, since it suggests that pressure drop can be reduced with no loss in heat transfer performance. There is a better comparison with the experimental results taking the misalignment of the deltas into account, which was a noticeable imperfection in the actual prototype. The goodness factor comparison has been updated to reflect the improved comparison in pressure drop between the delta-winglet fin and the louvred fins, and this is shown in Figure 7.5.3.

There has been some recent debate over the integrity of the RANS type turbulence models and in particular the $k-\varepsilon$ turbulence models. Their reliability with respect to highly turbulent flows, in comparison to the LES models is in doubt. The assertion is that the LES turbulence model produces the most accurate results. Therefore if one argues that an appropriately meshed LES model provides the highest level of accuracy, then it is astute to estimate the error incurred in using the $k-\varepsilon$ model, compared with using the LES model. In this manner the $k-\varepsilon$ model, can be used confidently with an error estimate attached. As a basis for comparison, the Flow-down delta-winglet (FDDW) configuration was chosen. This is because from observation of Figure 7.3.1 there is distinct vortex generation which is large in scale and hence more likely to be accurately simulated.

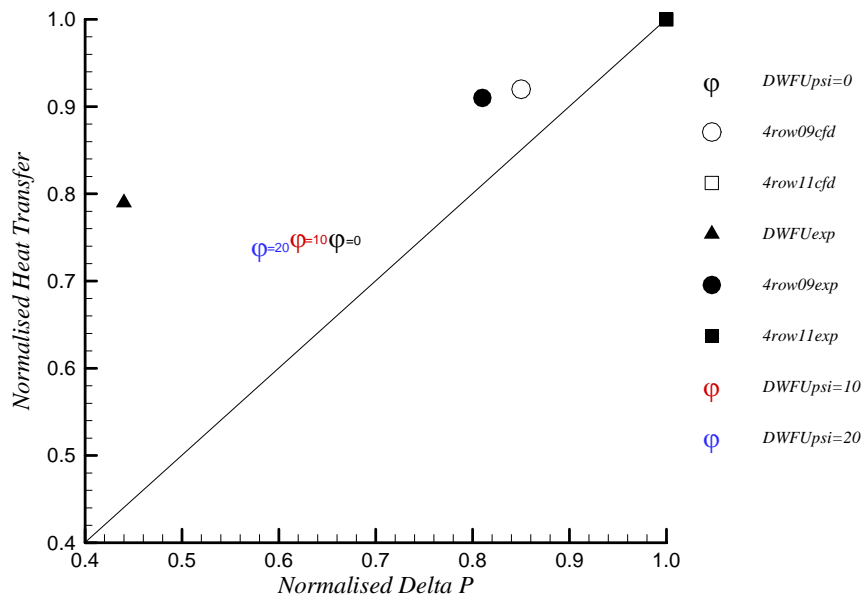


Figure 7.5.3 Simulated Goodness factor comparison of the Flow Up delta winglet at various angles of vertical offset angle (φ) and the lowre fin surfaces, with corresponding experimental results for CFD validation

An LES turbulence model as well as a Realizable $k-\varepsilon$ turbulence model were compared both graphically, for the appearance of flow features, as well as the calculated heat transfer and pressure drop results. Figure 7.5.5 and Figure 7.5.4 are comparisons of the results from the two simulations which display pathlines released from the surface of the delta-winglets. The pathlines have been coloured according to static temperature variation and hence give an indication of the heat transfer mechanism. The LES simulation shows the emergence of two distinct vortices issuing from the winglet. There is the main vortex shed from the leeward side of the winglet tip. The vortex has a diameter of approximately half the winglet height and the temperature is closer to that of the inlet air around 307K. Because it is shed from the winglet apex, it remains in the bulk flow somewhat above the fin surface. There is also a corner vortex rolling off the upstream side of the winglet/fin intersection. It has a diameter of approximately half that of the main vortex. Since it forms at the winglet/fin intersection it has a lower average temperature of about 290K and remains closer to the fin surface. Unfortunately neither of these vortices is ideal for optimum convection enhancement. Although the larger vortex is at a higher temperature, it is unable to

convey this high temperature fluid to the fin surface since it remains in the bulk flow remote from the fin surface.

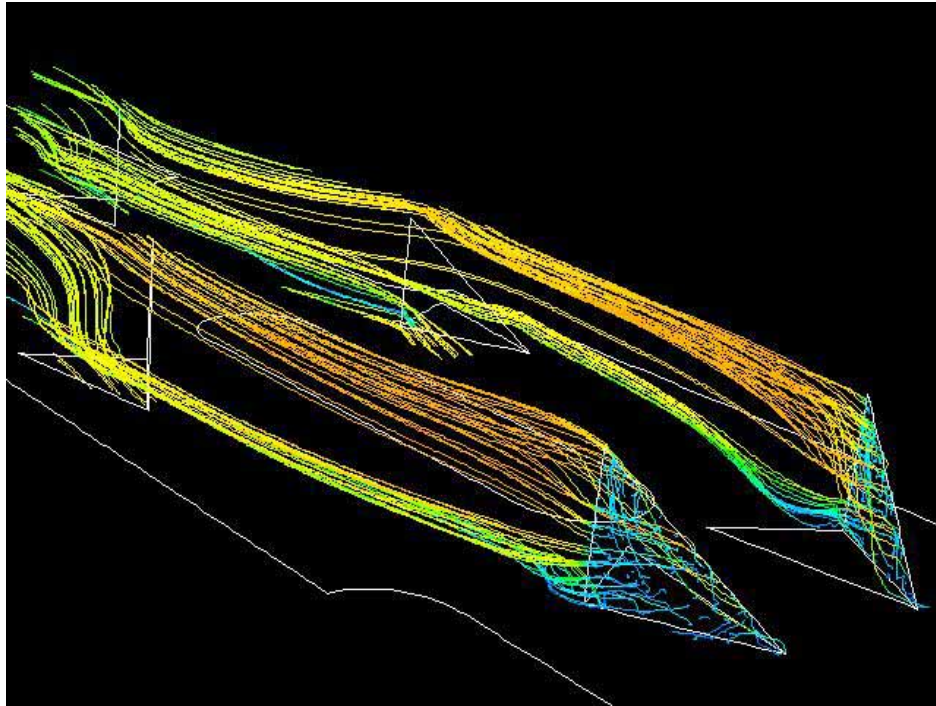


Figure 7.5.4 Pathlines released from the delta surface of the FDDW vortex generator at an inlet velocity of 6.3m/s. Realizable $k-\epsilon$ simulation

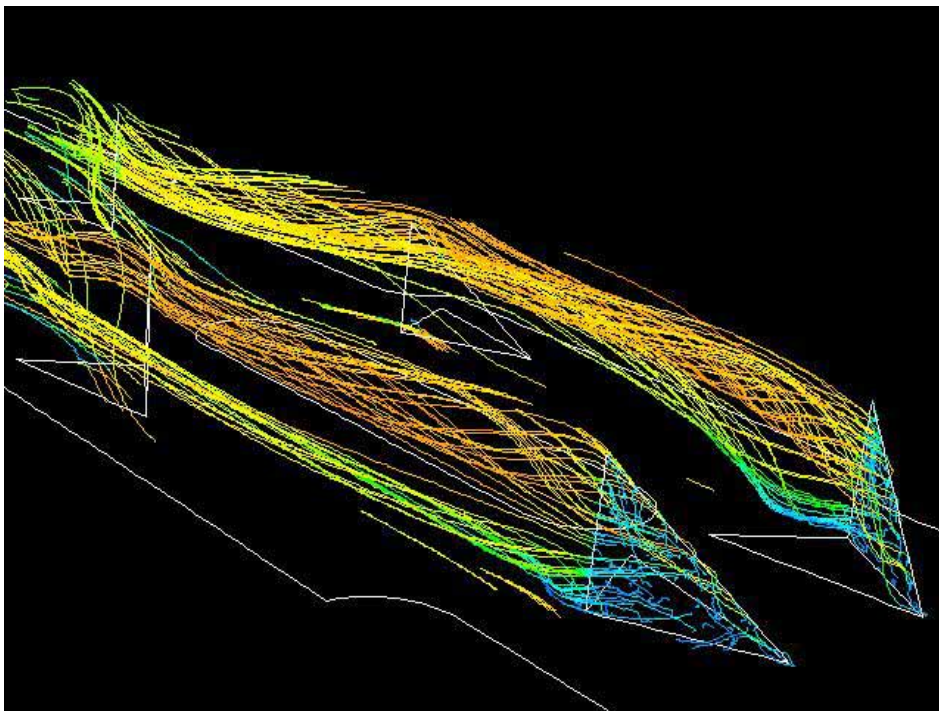


Figure 7.5.5 Pathlines released from the delta surface of the FDDW vortex generator at an inlet velocity of 6.3m/s. LES simulation

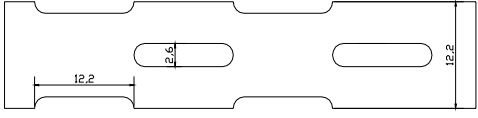

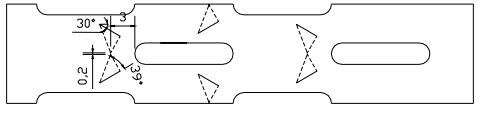

The smaller vortex has a closer proximity to the fin surface, but the temperature difference between the vortex and fin surface is not as great. This coupled with its small size hinders its potential to significantly improve heat transfer enhancement.

The Realizable k - ϵ model also determines the presence of the two vortices. However by comparing pathlines generated in Figure 7.5.5 and Figure 7.5.4, it can be seen that the LES model has identified far more rotational detail in the flow features while in the k - ϵ turbulence model they are less obvious. The calculated heat transfer for the steady state and RMS values are 4.01W and 4.00W respectively. This close agreement gives further confidence in the results obtained from the realizable k - ϵ simulations. It also implies that the vortex structure in this case is not a dominating influence over the overall heat transfer performance.

7.5.2.2 Comparison with plain fin geometry

Table 7.3 displays the performance comparison results of the FUDW vortex generator enhanced fin, and a plain fin surface simulation.

Table 7.3 Simulation comparison of a plain fin and the FUDW vortex generator enhanced surface

Plain versus FUDW	Fin temperature contours	\dot{Q}	ΔP
 <p>Plain Fin</p>		1.00	1.00
 <p>Delta Winglet Flow Up: x=-3mm</p>		1.23	1.27

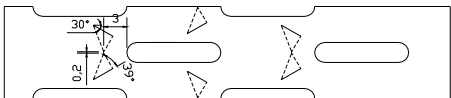

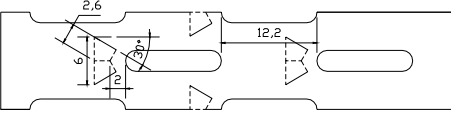

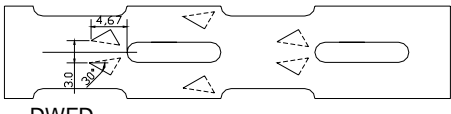
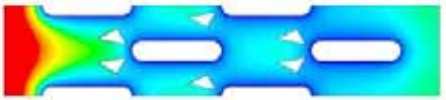
The results have been normalised with respect to the plain fin. The FUDW surface has enhanced heat transfer by 23%, but has also increased the pressure drop by 27%. The heat transfer enhancement compares remarkably well with those of Torii[9] and Kwak[10], who experimentally achieved a heat transfer enhancement of up to 30%

with delta-winglet vortex generators arranged in the tube wake, in a flow-up configuration. However, their configuration also resulted in up to a 55% *reduction* in pressure loss. Clearly, the reason for the low pressure loss is due to the fact that they had one row of winglets located behind the first tube row only. The equivalent heat transfer enhancement from a surface with a single row of winglets² seems to demonstrate that any downstream vortex generators provide very little additional contribution to heat transfer enhancement and serve mainly to increase pressure drop.

7.5.2.3 Comparison with Quad-shaped turbulence generators and Flow-Down Delta Winglets

Table 7.4 compares the results obtained from simulations of the quad shaped turbulence generator originally proposed, the flow down delta winglet, and the flow up delta winglet.

Table 7.4 Simulation comparison of Quad shaped Turbulence Generators and Flow Down Delta Winglets

Vortex Generator Type	Fin temperature contours	\dot{Q}	ΔP
 <p>Delta Winglet Flow Up: x=-3mm</p>		1.00	1.00
 <p>Quad Shaped Turbulence Generator</p>		1.08	1.37
 <p>DWFD</p>		0.96	0.77

The quad shaped turbulence generator has slightly higher heat transfer performance but a large increase in pressure drop. The high pressure drop is undoubtedly caused by

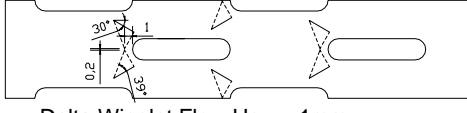

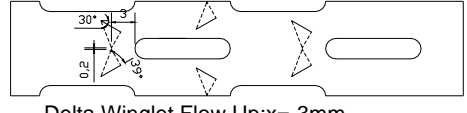
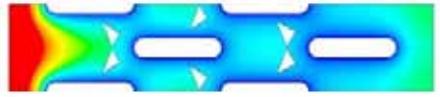
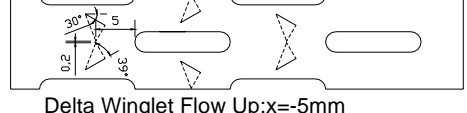

² The details of the findings of Torii and Kwak can be found in Section 2.2.2.7

the formation of separation zones in the generator wake, as was clearly observed from the flow visualisation results. The flow down delta winglet has slightly lower performance, but a much lower pressure drop. In this case the low pressure drop is due to the orientation of the winglets with respect to the tube which provides much greater flow clearance. This lack of imposition on the flow direction is also why the heat transfer performance is measurably lower.

7.5.2.4 Sensitivity to displacement of Delta Winglet in the x -direction

The distance of the delta winglet vortex generators from the tube stagnation point was chosen through an educated guess of the vortex path and its interaction with the tube. In the prototype this dimension which is along the x -axis was set at 3mm. A variation in both heat transfer performance as well as pressure drop can be expected with the variation of distance of the delta winglets from the front of the tube. Table 7.5 summarises the results of these simulations.

Table 7.5 Simulation comparison of Delta Winglet performance sensitivity to x position variation

Distance ($-x$) mm	Fin temperature contours	\dot{Q}	ΔP
 <p>Delta Winglet Flow Up: $x=-1$mm</p>		1.03	1.35
 <p>Delta Winglet Flow Up: $x=-3$mm</p>		1.00	1.00
 <p>Delta Winglet Flow Up: $x=-5$mm</p>		0.99	0.91

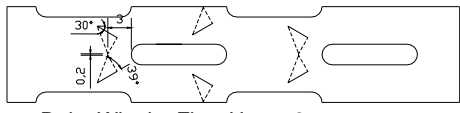

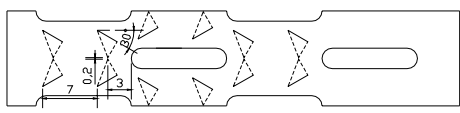

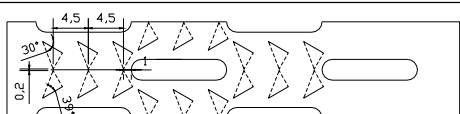

The heat transfer performance increases as the delta winglets are positioned closer to the tube stagnation point, and so does the pressure drop. This is in line with the

original predictions, since the fluid is guided onto the tube stagnation point. The improvement in heat transfer is as a result of increasing velocity gradients in this region. Increase in velocity gradients is accompanied by an increase in pressure losses. Similarly, as the delta winglet is positioned further from the stagnation point, both the capacity and pressure loss decrease.

7.5.2.5 Multiplication of Vortex Generators

The comparatively low pressure drop of the delta winglet fin suggests that additional rows of delta winglets may be added before the pressure drop exceeds that of the louvre fin coils. Simulations were performed in order to predict the effect of one, two and three sets of delta winglets located in the fin area in front of each tube. The results are shown in Table 7.6.

Table 7.6 Simulation comparison of performance prediction of multiple rows of Delta Winglets

Delta winglet rows	Fin temperature contours	\dot{Q}	ΔP
 <p>Delta Winglet Flow Up: x=-3mm</p>		1.00	1.00
 <p>DWFUFU</p>		1.05	1.23
 <p>DWFUFUFU</p>		1.11	1.69

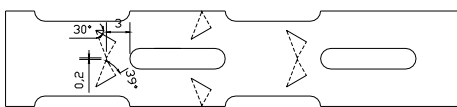

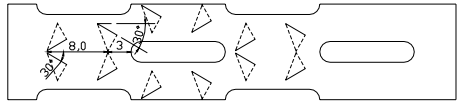

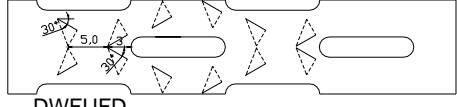

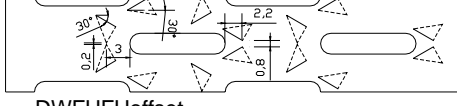

Doubling the quantity of vortex generators has produced a negligible increase in heat transfer but a 23% increase in pressure drop. Trebling the vortex generators has produced an 11% increase in heat transfer but a corresponding 69% increase in pressure drop. Additional vortex generators may increase the quantity of leading edges, but their effect on the vorticity and turbulence levels is unknown. On the one

hand, it is possible that turbulence levels should increase and hence improve heat transfer. But given the very minor improvement in heat transfer, this is unlikely to be the case. Rather there is strong suggestion that the stream wise vortices generated from one delta winglet may interfere with the vortices generated by another. Indeed, it is unlikely that well defined vortices will be generated from the downstream delta winglets which do not enjoy a uniform streamline flow field as do the first row of winglets. Furthermore, mechanical blockage may disrupt the vortex formation from the upstream winglets. Hence there is a strong possibility that any improvement in heat transfer due to the increase in leading edges is offset by the disruption of favourable convective flow fields. In addition the effectiveness of leading edges which are immersed in a highly turbulent flow field is questionable. By definition a leading edge causes the development of flow field, and hence unlikely to demonstrate any advantage in a flow field which is essentially fully developed. These reasons may explain why doubling or even trebling the quantity of vortex generators appears to show very little advantage.

7.5.2.6 Combinations of Flow-Up and Flow-Down delta-winglet Vortex Generators

It is apparent that locating the delta-winglets in symmetrical ordered rows proves to have little advantage in heat transfer performance, possibly due to their reciprocal interference. By alternating the orientation of the winglets, it is thought that there may be less interference between successive rows of winglets. Although numerous configurations were simulated all of them posed similar results. A selection of the better performing ones, have been presented for comparison in Table 7.7.

Table 7.7 Simulation comparison of various combinations of flow up and flow down vortex generators

Delta winglet rows	Fin temperature contours	\dot{Q}	ΔP
 <p>Delta Winglet Flow Up: x=-3mm</p>		1.00	1.00
 <p>DWFDFU</p>		1.07	1.31
 <p>DWFUFD</p>		1.02	0.99
 <p>DWFUFUoffset</p>		1.01	1.02

7.6 Goodness Factor Comparison

Finally all of the simulated results can be summarised in a comparative basis by displaying them in terms of the corresponding goodness factors shown in Figure 7.6.1. Note that the goodness factors above the unity line indicate favourable combinations which exhibit greater heat transfer with respect to pressure drop than the 4row11 louvre fin coil.

From Figure 7.6.1 it can be seen that there is no obvious pattern relating to the heat transfer and pressure drop of the various delta winglet surfaces. It seems that the fin surface with the best performance out of the delta winglets, is the DWFUFD surface but its performance falls short of the louvre fin coils. It has 77% of the heat transfer at 66% pressure drop of the 4row11 louvre fin surface. However its performance is only marginally better than the original flow up delta winglet fin surface

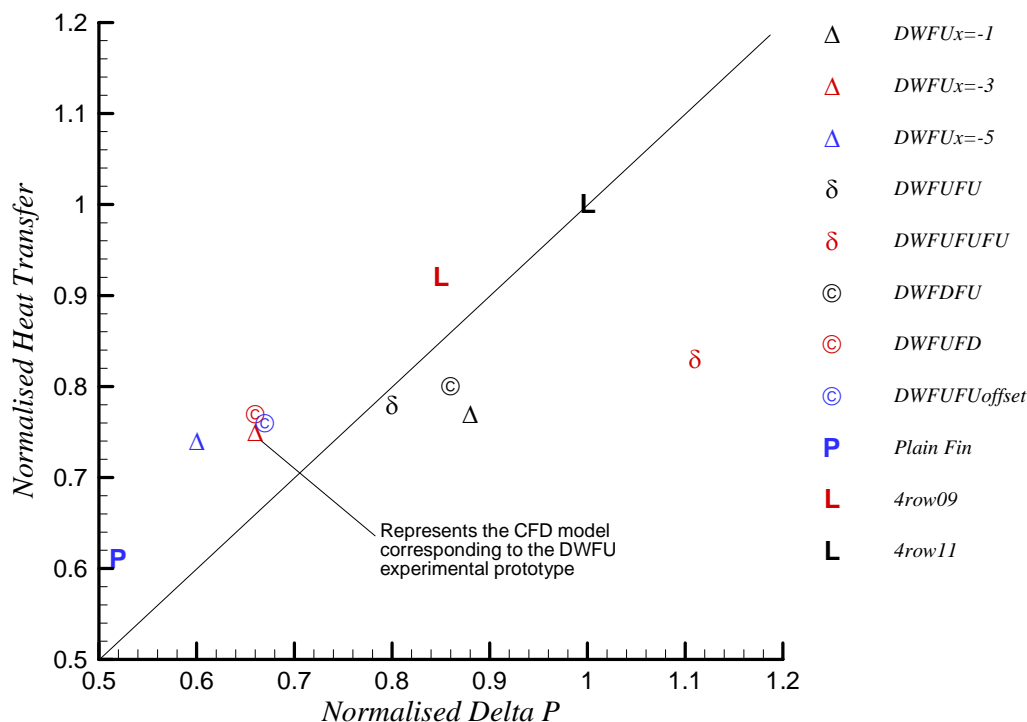


Figure 7.6.1 Comparison of simulated Numerical Goodness Factors between the various Delta Winglet configurations, and the standard louvre coils

7.7 Temperature variation through coil

In order to appreciate how effective each fin surface is in transferring heat, the temperature change of the air as it progresses through each coil was investigated. This was accomplished by calculating the average temperature across a vertical plane in each coil at various distances from the inlet face. The vertical surfaces were located at the front of each tube, so that by calculating the temperature difference between two successive planes, imparted the heat transfer contribution of that particular tube row. Note that the $x=0$ position corresponds to the second tube row stagnation point. The first ΔT is measured between the inlet air temperature and the temperature just before the first tube row. This then provides the heat transfer contribution of the leading edge of the fin, and so on. Figure 7.7.1 is a graph plotting these calculated results from the Numerical simulations of the two louvre fin coils and the delta-winglet Flow-Up vortex generator geometry.

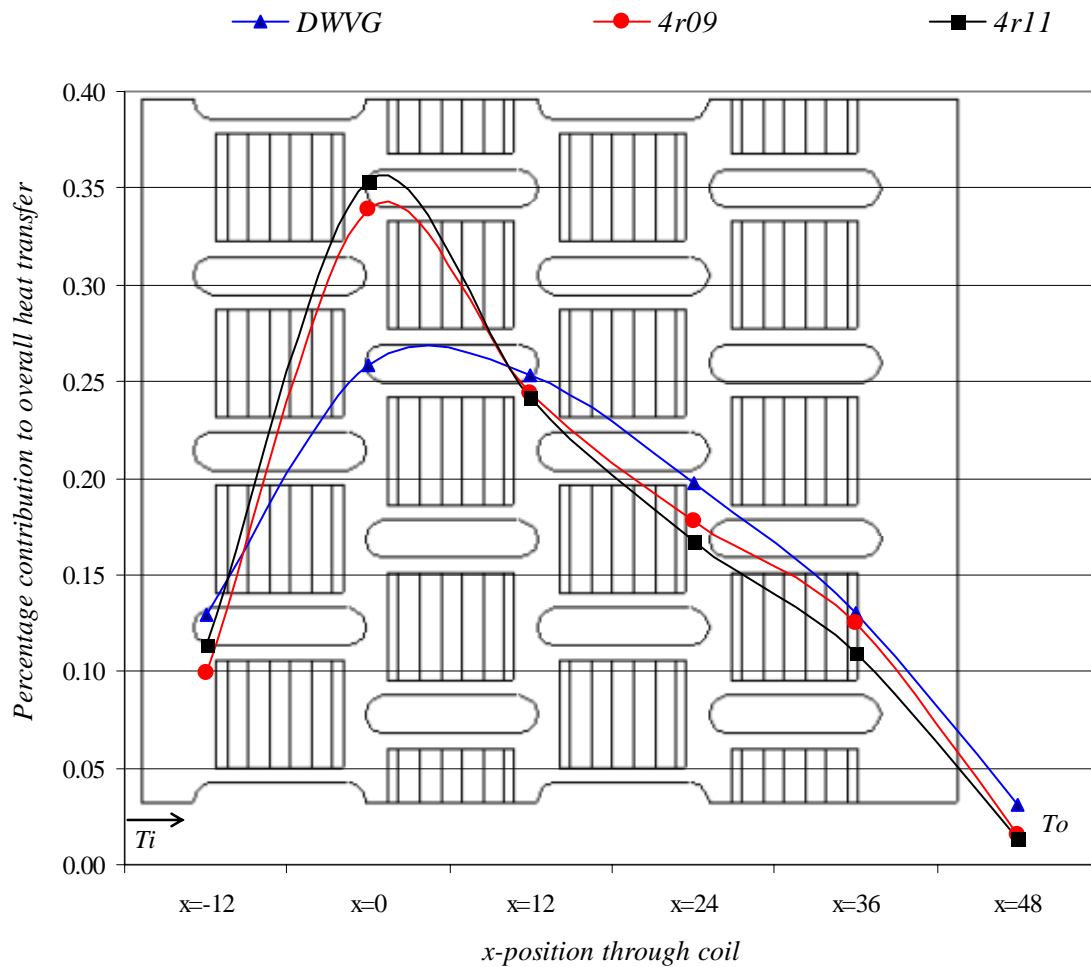


Figure 7.7.1 Graph plotting the % temperature change of the inlet air initially at T_i , at each x -position as it progresses through each coil

It is apparent that the leading edge of the fin only contributes about 12% of the total heat transfer in each case. Considering the louvre fin coils, almost half of the total heat is removed from the air by the time it has reached the end of the first tube row. The first tube row is the major contributor to the overall heat transfer, accounting for approximately 35% of the total heat transfer. The second tube row removes less than 25%. In the delta-winglet coil which has a lower overall performance, just over 25% is removed by the first tube row and the same for the second tube row. In each case the trailing edge of the fin contributes very little to the total heat transfer, less than 5%. These results indicate that in a high performance coil, the first tube row contributes

significantly more to the overall heat transfer than the following rows. This suggests that there is considerably more opportunity for heat transfer improvement in the downstream rows rather than at the front row which already appears to be at a local high.

7.8 Concluding remarks

The experimentally measured heat transfer performance of the delta-winglet surface was lower than that of the louvre fin surface by about 15%, when compared at the same fin density. On the other hand the delta-winglet surface had approximately half the pressure drop. These results seem to suggest that streamwise vortices in a global sense do not improve the overall airside heat transfer coefficient, although locally they may do so. Apparently the arrangement of flow-up delta winglets did not increase turbulence levels to enhance heat transfer sufficiently to be on a par with the louvre finned coils directly. However it was demonstrated that by increasing the coil face area by 15% the capacity would be equivalent to the louvre finned coil and the fan power consumption would only be 54%. This is an appreciable saving in fan power which could be seen to be an advantage over the increase in coil size.

It was also experimentally established that increasing the inlet air velocity by 30% to 8.2m/s, the delta-winglet coil has an equivalent heat transfer performance to the louvre coil having 9 *fpi* at only 89% of the air pressure drop.

Increasing the quantity of vortex generators does not greatly improve the results. Numerical simulations demonstrated that doubling or even trebling the quantity of vortex generators would have little additional benefit. This is because the additional vortex generators create additional flow disturbance which may disrupt the intended vortex structure. This may only result in an increase in turbulence in the bulk flow which is likely to increase pressure drop. As a result any localised enhancement at the fin surfaces due to coherent stream wise vortex generation may be compromised. Hence the interference caused by the increase in the quantity of vortex generators can actually be counterproductive. The prospect of increasing vortex generation and hence convection, by replacing louvres with winglets, with a consequent reduction in the quantity of leading edges, hinders heat transfer rather than enhances it.

Additional numerical simulations to investigate alternative combinations of flow-up and flow-down delta-winglets reinforced this conclusion. It seems that the most effective heat transfer mechanism in the confines of narrowly spaced plates when coupled with flat tubes is by boundary layer restarting, and this is most effectively achieved by a louvred surface.

The above reasoning may be valid for vortex generators which are geometrically of the same size as the fin spacing. Should the strength of the generated vortices increase by increasing the winglet size relative to the rest of the geometry, then improved results may occur. However, increasing the size of the winglets would necessitate increasing the fin pitch, and the consequent reduction in surface area may negate any improvement in heat transfer due to convection enhancement.

It was determined that the front end of a coil performs the greatest proportion of heat transfer. This implies that there is possibly more scope for improvement in heat transfer from the downstream rows rather than the first row which already experiences an apparent maximum.

Chapter 8

Effect of leading edges combined with stream wise vortices

8.1 Introduction

It was established fairly convincingly from Chapter 7, that delta-winglets, irrespective of quantity or configuration, do not enhance convection coefficients sufficiently in order to compete with a louvre fin surface. This is because louvres and winglets provide two different enhancement mechanisms. Louvres provide a multiplication of leading edges, while Winglets generate vortices which improve local convection levels. One can deduce that in a coil, the leading edge effect is more fortuitous in enhancing heat transfer than attempting to increase the convection levels. Within the confined spaces of the tube and fin geometry, achieving a suitable vortex type flow structure to adequately increase convection is challenging. Interference from the coil surfaces as well as adjacent vortices tends to disrupt the flow structure. Also, it seems that if the height of the winglets (which determines the scale of the vortices), is similar to the louvre width, then the amount of enhanced convection is insufficient to enhance heat transfer sufficiently to equate to the enhancement provided by the leading edges of the louvres. Even if the winglets are combined with louvres, the scale of the vortices is roughly equivalent to the louvre height, so that disruption and breakdown of the vortex structure occurs as it negotiates the louvre surfaces. As a result little improvement in heat transfer occurs. This was experimentally demonstrated by Lozza and Merlo[12], as discussed in Section 2.2.2.8.

On the other hand, if the scale of the vortices are much bigger than the louvre height, they may have sufficient energy and momentum levels to be unaffected by the louvre surfaces. Also, if the vortices are generated some distance above the fin surfaces then they may be able to avoid the louvre edges altogether. Or ideally the outer radius of

the vortex will just coincide with the edges of the louvres, and therefore provide maximum convection and disruption to the boundary layers developing on the louvre surfaces. This concept is sketched diagrammatically in Figure 8.1.1. The purpose of the current study is to investigate potential heat transfer enhancement by combining the two mechanisms, namely multiple leading edges and streamwise vortices.

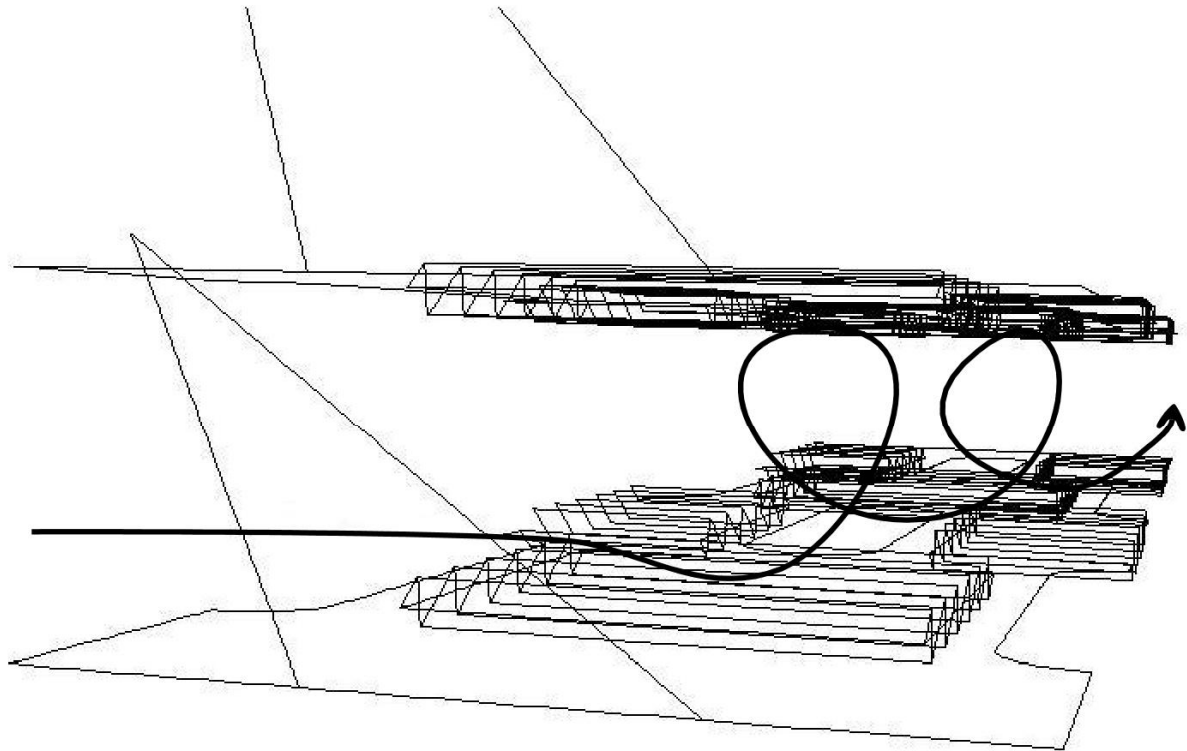


Figure 8.1.1 Sketch of desired vortex development in a delta enhanced louvre fin combination

8.2 Proposed Delta Configurations

Jaorder and Jacobi[11] achieved tremendous results (up to 21% heat transfer improvement) by placing a delta wing on the leading edge of the fin surface. However their analysis centred on triangular duct fins in a serpentine arrangement and is therefore geometrically far removed from the parallel fin arrangement focused on here (Refer to Figure 2.2.12. for a comparison). The relatively large area of the triangular ducts provides an open geometry for the generated vortices to develop. The narrow fin spacing inherent in parallel fins limits the possibility of inserting a delta of reasonable

dimensions. However, doubling the fin spacing of the 4row11fpi coil to achieve 5.5fpi may provide sufficient fin clearance to accommodate a reasonably sized delta wing. Also, widening the fin spacing will allow more room for vortex development and longevity. This fin spacing is commonly used in some applications and hence an improvement in heat transfer for such coils would be of benefit. It is not a requirement that the delta wing participate in heat conduction, since its primary function is to generate large vortices. This means that the delta wings could typically be fabricated from plastic and moulded on a continuous strip for easy insertion onto the leading edge of each fin. In addition, these “inserts” could possibly be retrofitted onto existing coils, increasing the range of application.

Several Delta profiles were considered for the Numerical study. Since the profiles had to be accommodated within the fin spacing, the delta height was kept constant, and equal to the fin spacing. Therefore the delta chord length was varied in accordance with the varying angle of incidence α . Hence chord length C_L varied from 2 times the fin pitch F_p having a shallow angle of incidence $\alpha=30^\circ$ degrees, to $1.5F_p$ and $\alpha=42^\circ$, through to $C_L=F_p$ and $\alpha=90^\circ$ degrees. While there are many configurations that may have been adopted, this selection covers a sufficient range to trial the principle, rather than provide any form of optimisation. The various delta profiles are illustrated schematically in Figure 8.2.1.¹

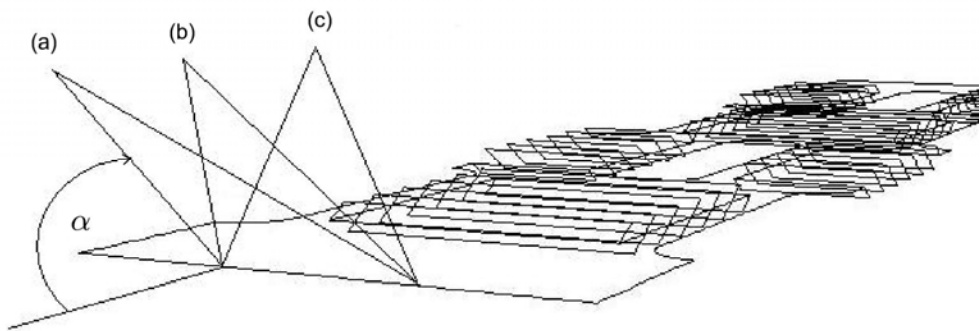


Figure 8.2.1 Sketch of the proposed Delta Wing vortex generators combined with a louvre fin surface for the case of a) $C_L=2F_p, \alpha=30^\circ$, b) $C_L=1.5F_p, \alpha=42^\circ$ and c) $C_L=F_p, \alpha=90^\circ$

¹ The Delta profile proportions of Joarder and Jacobi can be obtained from Figure 2.2.12

8.3 Numerical Procedure

A series of CFD simulations were performed in order to investigate the possibility of enhancing heat transfer by combing Delta Wings which are large in comparison to the louvre height. Note that the louvre height is 0.375mm for a louvre angle of 30° compared to the fin pitch of 4.62mm.

8.3.1 Computational Domain

The computational domain for this series of simulations was similar to those presented in the previous chapters. However, in line with the increase in fin pitch, the width of the model was increased to 4.62mm, which is equivalent to 5.5fpi. In addition to the delta/louvre combinations, a louvre fin surface without a delta was included to improve the accuracy of the comparisons. Figure 8.3.1 is a sketch of the typical mesh structure used for the Delta/Louvre combinations.

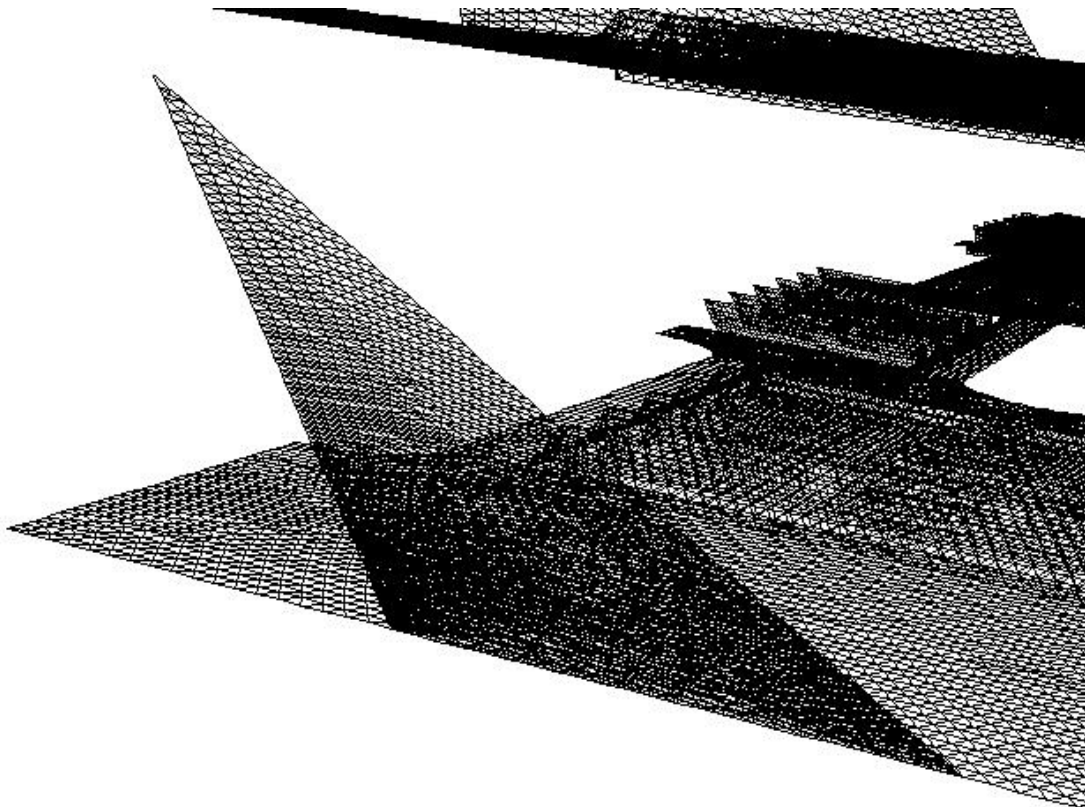


Figure 8.3.1 The typical mesh structure for the series of Delta-Wing geometries combined with the louvre fin surface

8.3.2 Boundary Conditions

The identical boundary conditions were used as in the previous simulations. Only the maximum velocity of 6.3m/s was specified at the inlet boundary for each model since the lower velocities showed a direct (almost linear) relationship with this case. The top, bottom and side boundaries were specified as periodic. This was particularly crucial for the side boundaries which were heavily influenced by the presence of the deltas.

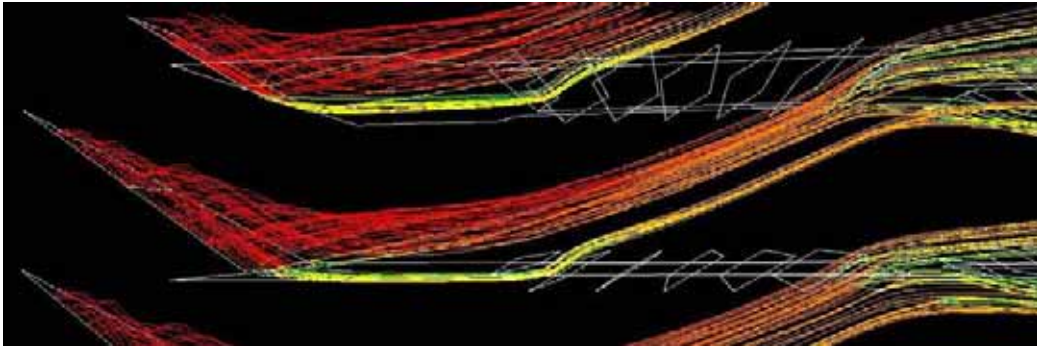
8.3.3 Numerical Results

The models were tested successively from the case of a plain louvre fin with no delta, through $\alpha=30^\circ$, $\alpha=42^\circ$ to $\alpha=90^\circ$. The results initially indicated that irrespective of Delta configuration, the presence of the deltas provided no significant enhancement in heat transfer, although the pressure drop increased with increase in α . In order to understand why this was the case, the flow path line trajectories were plotted in order to establish whether stream wise vortices were present, and if so, how they interact with the fin surfaces. Figure 8.3.2 shows the resulting path lines for each case. The path lines have been coloured using static temperature (the temperature that is measured moving with the fluid) as the variable. Therefore the variation in temperature of the air as it progresses through the heat exchanger can be distinguished.

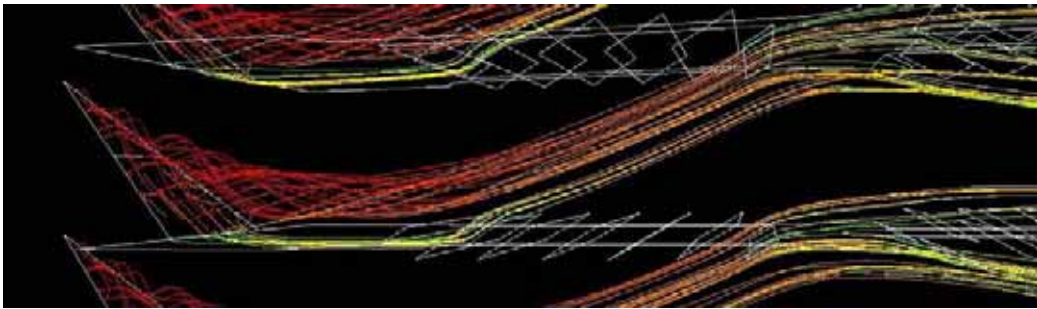
In the case of $\alpha=30^\circ$, Figure 8.3.2 a), there are stream wise vortices developing from the delta surface but the scale of these vortices is small, having a diameter of about $0.25F_p$. Initially they travel downstream parallel to the fin surface, however as they cross the louvre edges they encounter high velocity flow issuing upwards from the between the louvres. They are swept upwards, towards the louvres in the adjacent fin, and pass between the last few louvres of that set.

In the case of $\alpha=42^\circ$, Figure 8.3.2 b), the scale of the stream wise vortices is slightly larger, having a diameter of about $0.3F_p$. The vortices are still swept upwards to pass through the rear of the adjacent louvres as before.

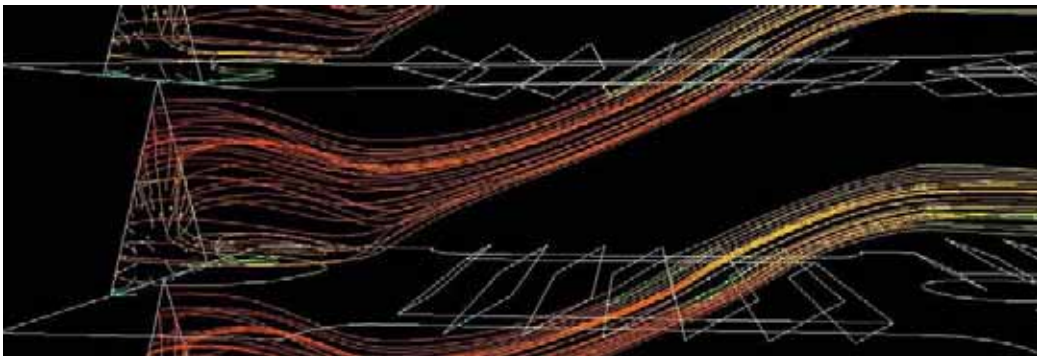
When the Delta angle is perpendicular to the fin edge, the vortices are larger still, having a diameter of about $0.4F_p$, and they are no longer stream wise but more transverse, rotating in a horizontal plane behind the Delta. They have less stream wise momentum and are rapidly swept upwards to pass through the adjacent louvres but this time towards the centre of the louvre set.



(a) $CL=2F_p$, $\alpha=30^\circ$



(b) $CL=1.5F_p$, $\alpha=42^\circ$



(c) $CL=F_p$, $\alpha=90^\circ$

Figure 8.3.2 Pathline trajectories of vortex development for each Delta-Wing combined with louvre configuration at $Re_{D_c}=1076.32$. The pathlines have been released from the Delta surfaces, and are coloured according to static temperature.

Hence the longevity of the vortices is minimal and is determined by the influence of the high momentum flow through the louvres. As the vortex is swept through the adjacent louvres, the rotational velocity is quenched. This is undoubtedly why the vortices appear to have minimal impact on the heat transfer performance. A similar effect would be seen at lower inlet velocities since as the louvre directed flow is decreased, the vortex strength will also decrease.

The vortices are initiated by the high velocity inlet flow swirling into the low pressure zone behind the delta. Due to the incline of the Delta towards the flow, the low pressure zone occurs above the Delta surface. Hence the approaching flow is deflected upwards towards this low pressure zone as it passes the Delta edges. This also contributes to the upward displacement of the vortices towards the adjacent louvres. It may be possible that if the lean of the delta was away from the approaching flow rather than towards it, then the low pressure zone should be smaller, and below the Delta surface. This may encourage the flow downwards, so that it offsets the influence of the high momentum flow issuing through the louvres. Hence another delta configuration was trialled, which had an angle of incidence $\alpha=138^\circ$ or 42° measured from the fin surface. In this case because of the shallow angle, the chord length could be lengthened to $1.5F_p$. Figure 8.3.3 shows the pathline trajectories for this configuration.

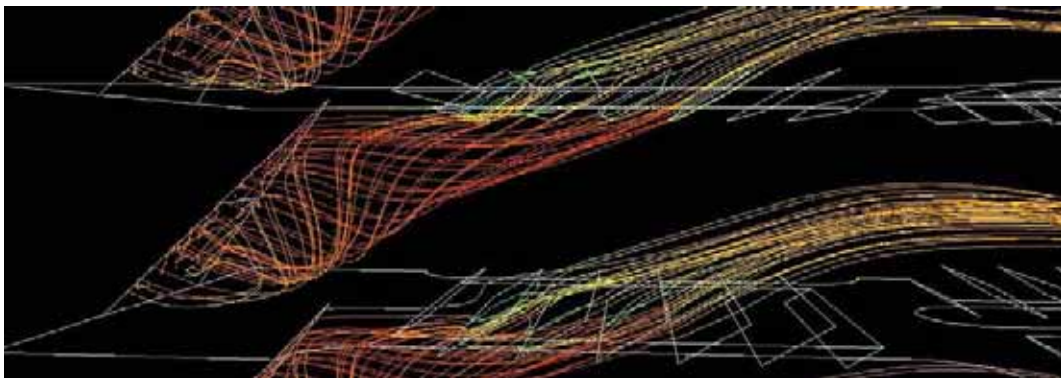


Figure 8.3.3 Pathline trajectories of vortex development for Delta-Wing combined with louvre configuration having $\alpha=138^\circ$, $Re_{Dc}=1076.32$

The scale of the vortices developing behind the Delta, are approximately $0.5F_p$ in diameter. The stream wise momentum is very low and the vortices are immediately swept upwards and pass through the adjacent fin louvres towards the front in this case.

It was observed by looking at the entire flow field in this last case, which after the vortex had passed through the first row of louvres, it doesn't entirely disappear. It seems to re-establish some weak circular motion and then incongruously continues downstream in a stream wise fashion but between the adjacent set of fins from where the Delta is located. Figure 8.3.4 shows the development of this circular stream wise motion.

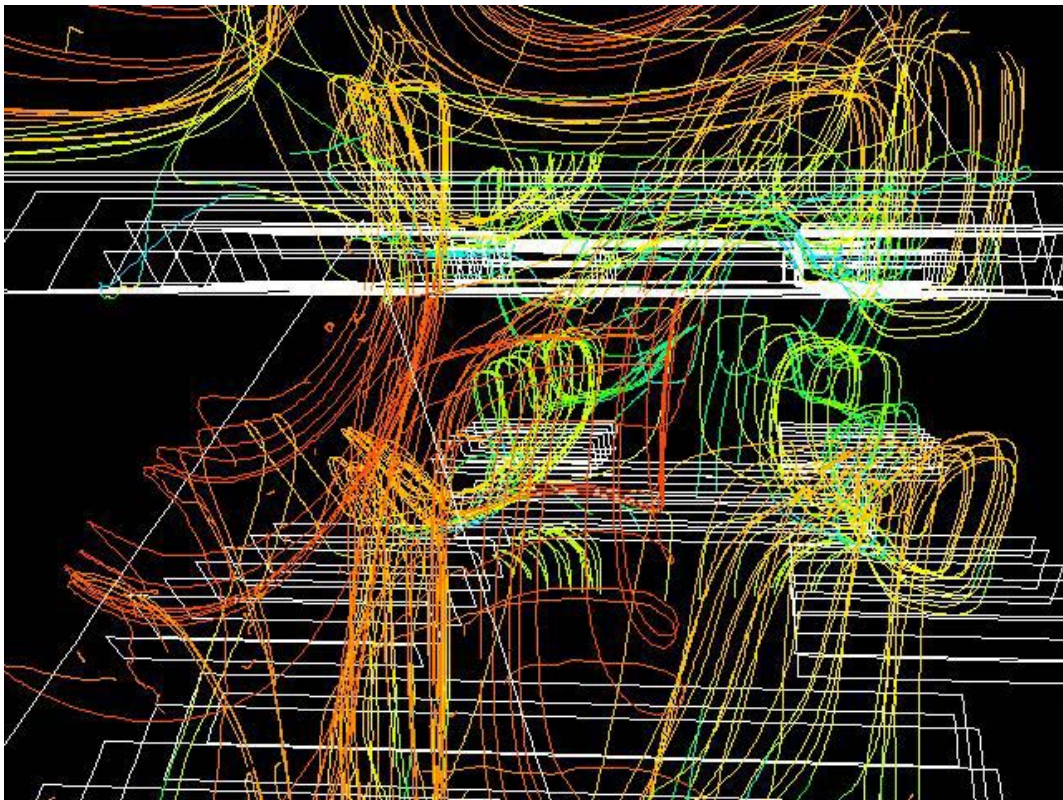


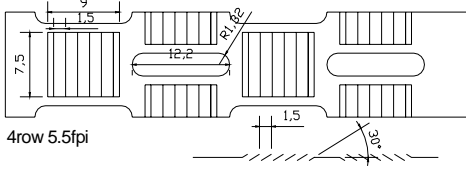
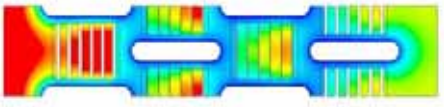
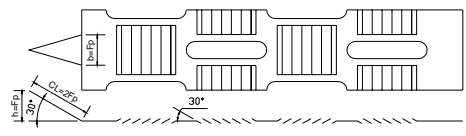
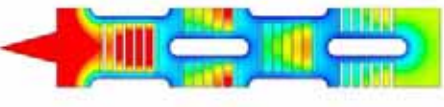
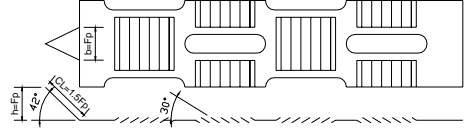
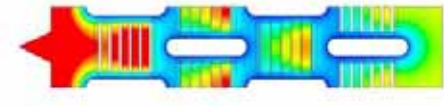
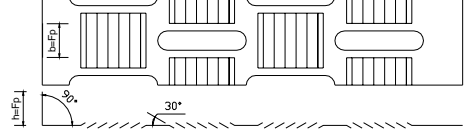
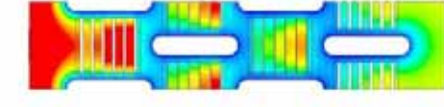
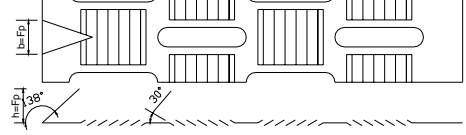
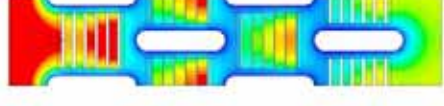
Figure 8.3.4 Shows a view of the pathlines for $Re_{D_c}=1076.32$ looking in the downstream direction.

The path lines have entered from below through the louvres in the foreground, and then continue downstream in a weakly circular trajectory. They are swept along by

the bulk fluid flow and appear to have no interaction with the louvre surfaces. Hence they do not appear to provide any significant heat transfer enhancement.

The overall results² for this set of simulations comparing heat transfer performance and pressure drop is tabulated in Table 8.1 which shows the normalised performance comparison between the louvre surfaces combined with delta-wings, as well as the standard louvre surface, all having 5.5fpi.

Table 8.1 Numerical performance comparison between the standard louvre fin surfaces at various fin pitch, versus the combined Delta/louvre surfaces at 5.5 fins per inch

Louvre plus Delta	Fin temperature contours	\dot{Q}	ΔP
 <p>4row 5.5fpi</p>		1.00	1.00
		1.01	1.04
		1.01	1.06
		1.01	1.12
		1.01	1.11

² The simulated performance comparison showed that the standard 5.5fpi louvre coil had a maximum capacity of 68% of that of the 11fpi louvre coil. A comparison with proprietary louvre coil data for the 5.5fpi coil showed that it had about 70% of the 11fpi capacity determined experimentally, and hence gives further validation to the Numerical results.

From Table 8.1 it can be seen that there is negligible improvement in heat transfer in each case. There was also a slight increase in pressure drop which generally increased with increase in the angle of incidence from 4% up to 12%.

8.4 Concluding Remarks

The Numerical simulations indicated that the presence of a large Delta-Wing did not result in any significant improvement in heat transfer performance, while there was a slight increase in pressure drop. It is apparent that the scale of the vortices was not large enough to span between the fins, and hence lacked rotational energy. In addition interference from the strong louvre directed flow which had sufficient momentum to deflect the vortices from a stream wise direction and force them through the adjacent fin louvres, further weakened their rotational momentum. The scale of the vortices was seen to increase as α increased. However, as the scale of the vortex increased its stream wise momentum decreased, so that it was more easily diverted by the louvre directed flow.

These results are poor when compared to those achieved by Jaorder and Jacobi[11] who demonstrated experimentally an improvement in heat transfer performance of 21%. This can be explained by considering the air inlet velocities that were used. They conducted their experiments using air side Reynolds numbers based on hydraulic diameter between 200-500 which they claim is the typical range for automotive applications. This range of Reynolds number is far lower than used in the numerical simulations performed here. Using the same definition of Hydraulic diameter as opposed to tube collar diameter the Reynolds number for the simulations is 2472 or 5 times as large. At low Reynolds number the flow is more likely to be duct directed rather than louvre directed. So while it is possible to achieve large enhancements in a flow that is duct directed, it defeats the object of having louvres since louvres are only effective if the flow is louvre directed. If the Reynolds number is increased to achieve louvre directed flow, this causes the vortex structure to be compromised because it is swept in between the louvres as seen from the simulations. In short it can be said that a delta combined with a louvre surface will only produce heat transfer enhancement at low Reynolds numbers for which the flow is duct directed.

The simulation results are more in line with those obtained by Lozza and Merlo[12], as discussed in Section 2.2.2.8. They found that 4 delta winglets in combination with louvres on parallel plate fins actually had poorer heat transfer performance than other louvred surfaces.

On the other hand, the results are not that surprising considering what was established in the Chapter 7. It was demonstrated that the bulk of the heat transfer is removed from the first tube row. Since the heat transfer from this zone is already at a maximum, it was concluded that very little improvement can be gained by trying to enhance convection. One could extend this summation to include that in the current tube fin geometry, leading edge vortex generators provide little chance of heat transfer enhancement.

Chapter 9

Louvre Fin Design and Optimisation

9.1 Introduction

The louvre fin design has distinct advantages over other enhanced fin surfaces. The number of leading edges obtainable per unit area is at a maximum from a logistical aspect, as well as from the ease of manufacturing. Typically the louvres are pressed out of the fin surface by a combined cutting and rolling action. Because of the louvre angle, the louvres can be stacked closer to one another resulting in smaller louvre pitches. In comparison, the strip fin or offset strip fins are parallel to the fin surface, and therefore the pitch is determined by the strip width. In the case of the offset strip fin for example the strip pitch is twice the strip width.

The enhanced performance of a louvre surface is directly attributable to the increased number of leading edges, rather than the level of turbulence generated. Clearly the quantity of leading edges obtainable is related to the geometry. However, for a fixed quantity of louvres, the louvre angle should influence the heat transfer performance, and pressure drop. The effect of louvre angle on coil performance may not be generalised, but has been shown to be specific to a particular coil design, depending on the number of tube rows, and tube profile as well as other geometric configurations. Hence the effect of varying the louvre angle on the performance of the current louvre fin geometry may not be intuitively predicted. The flow transition from duct directed to louvre directed further complicates predictions. Therefore in order to predict the affect of louvre variation on coil performance it is essential to perform a coil specific investigation. In this chapter the effect of varying louvre angle as well as louvre quantity is examined for the current coils of interest. In addition the prospect of louvre enhancement by serrating the edges will be investigated. This is a unique endeavour which has hitherto not been suggested. Finally, the concept of shifting the heat

transfer emphasis from the front tube row so that more of the heat exchanger surface is more effectively utilised is considered. This is achieved by varying the louvre angle from shallow at the front to much steeper at the rear. The investigation was performed by a comparative Numerical study. The reliability of the CFD models has been proven through the previously reported comparison of similar models with experimental results. The numerous variation of geometric parameters required makes prototype evaluation virtually impossible. Clearly the difficulties of prototype fabrication of louvred fin surfaces can be appreciated. Modifying some of the geometrical parameters suggested here would require a major investment in retooling that may not be justified even if a (slight) performance improvement can be proven.

9.2 Background

Leu et al[51] performed a numerical investigation to predict the effect on a two row coil performance of varying the louvre angle(θ), louvre pitch(L_p) as well as louvre length(L_L). Their results are particularly relevant to the present study since their numerical model included oval tubes. They found that the air pressure drop increases with increase in θ for all L_p and the increasing trend is especially significant at smaller L_p . Also the smaller L_p would result in better heat transfer performance. This is attributable to the periodic renewal of the boundary layer. The relationship between θ and the average Nusselt number is far more complex. They observed a “maximum” phenomenon of average Nu with change in θ , as shown in Figure 9.2.1.

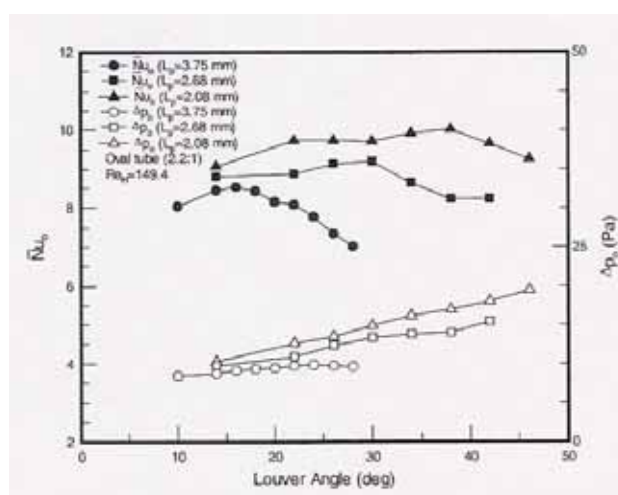


Figure 9.2.1 Heat transfer performance and pressure drop vs louver angle for three specific louver pitches. Reproduced from Leu et al [51]

This phenomenon was particularly distinctive at the largest L_p . Also the Θ at which the maximum phenomenon occurs, increases with decrease in L_p . It was observed that boundary layers exist on both the upper and lower surfaces of the louvre surface. The relevant heat transfer enhancement is due to the thin boundary layers that form at the leading edge of each louvre. Apparently the development of the boundary layer on the upper and lower surfaces should be different due to the presence of the louvre angle. Due to the impinging airflow, the upper surface will experience a thinning of the boundary layer while the wake side of the louvre will experience a thickening of the boundary layer which actually impedes heat transfer along this surface. This thickening of the underside boundary layer also increases with louvre angle. Hence the resultant heat transfer performance is the summation of the contributions from the upper and lower surfaces which may result in a maximum at a particular louvre angle.

DeJong and Jacobi[78] performed mass transfer and pressure drop comparisons as well as complimentary flow visualisation on louvred arrays at various fin pitch and louvre angle. The louvred arrays did not include tubes, and therefore may have significantly different results than if the presence of tubes was included. They noticed that at a critical Reynolds Number, the leading edges of the arrays were seen to shed small vortices. The mass transfer measurements indicated that these vortices did not provide any significant heat transfer enhancement. They noted that a 10° increase in Θ from 18° to 28° increased heat transfer by 25-35%, but also increased pressure drop by approximately 100%. This dramatic increase is clearly due to the comparison with a very gentle louvre angle of 18° . The louvre angle of the louvre fin surfaces studied in this report was steep at 30° and therefore only subtle increases in louvre angle can be accommodated.

9.3 Procedure

A CFD investigation using the previously developed louvre fin geometry having $9fpi$ as a comparison basis has been performed. The geometry has been modified to investigate the effect of varying Θ , as well as varying L_p . Values of Θ of 25 degrees and 35 degrees have been compared to the standard Θ of 30 degrees. The simulations were performed using the maximum inlet velocity of 6.3 m/s .

By varying the L_p , the effect of varying the quantity of leading edges on performance may be investigated. An L_p of 1.25mm and 1.875mm are compared with the standard L_p of 1.5mm . In order to make these comparisons meaningful, an equivalent louver area has been maintained in the three cases. This is warranted by the fact that the available fin area available for location of the louvres is restricted to the spaces between the tubes and therefore is essentially fixed. Of course reducing L_p by increasing the quantity of louvres within the same area of fin requires that the louver width be correspondingly shorter since the louver width is also equal to L_p . Similarly increasing L_p by reducing the number of louvres requires that the louver height be correspondingly higher for the same Θ . To illustrate these differences in the various geometries, Figure 9.3.1 has been included which shows a portion of the meshed louver area in each case.

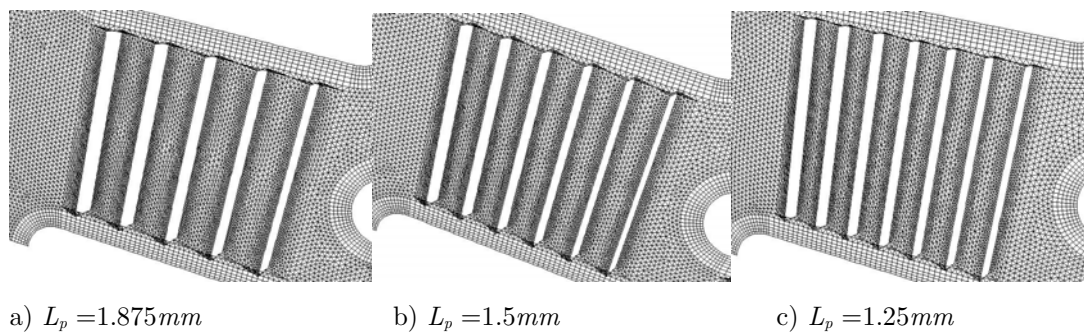


Figure 9.3.1 Sketch showing the extent of the louver area for each of the louver pitches

Strictly speaking, a slight discrepancy exists in louver area between the three cases if the landing width of the louvers is taken into account. The landing width is equal to $L_p/2$. The landing width for the case of an L_p of 1.25mm (6 louvers) is 0.625mm wide, and for an L_p of 1.875mm (4 louvers) it is 0.9375mm wide, as opposed to 0.75mm wide for the case of an L_p of 1.5mm (5 louvers). Since there is a variation in landing width in each case, a slight discrepancy in total louver area exists. The differences in louver area as a ratio of the standard case are 0.97 for the case of 6 louvers, and 1.04 for the case of 4 louvers. This area ratio has been applied to the heat transfer results as a

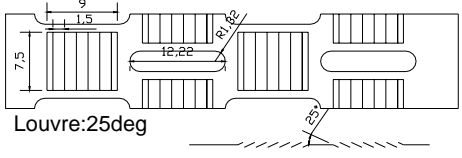
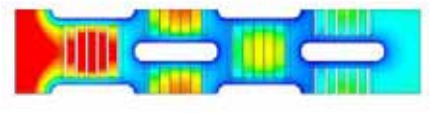
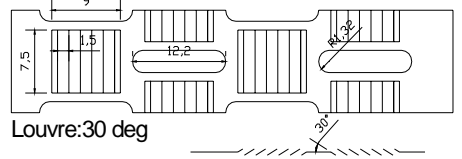
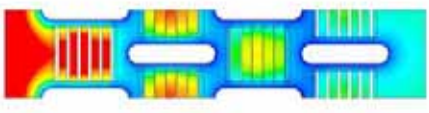
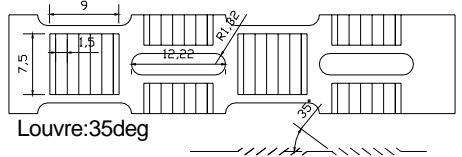
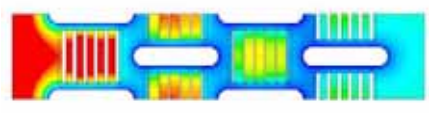
correction factor¹. In all cases the L_L has been kept constant since this parameter is determined by the transverse tube pitch and is therefore also essentially fixed.

9.4 Results

9.4.1 Effects of Louvre angle variation

Table 9.1 summarises the performance results due to variation of θ by 5 degrees in each direction from the standard angle of 30 degrees. The results have been normalised with respect to the standard case of 30 degrees.

Table 9.1 Louvre fin performance comparison at 9 fpi with varying louvre angle and constant louvre pitch of 1.5mm

Louvre angle (θ)	Fin temperature contours	\dot{Q}	ΔP
 Louvre:25deg		0.99	0.88
 Louvre:30 deg		1.00	1.00
 Louvre:35deg		1.01	1.17

It is evident from these simulations that a 5 degree variation in θ has very little effect on heat transfer performance. There is a slight decrease in heat transfer with reduction in θ and a miniscule increase in heat transfer with increase in θ , as is reflected by the minimal variation in fin surface temperatures. There is a much greater variation in pressure drop however, a 12% reduction with decrease in θ and a 17% increase in pressure drop with increase in θ . The absence of significant variation in heat transfer

¹ The application of this correction factor is based on the assumption that the majority of heat transfer is performed by the louvers.

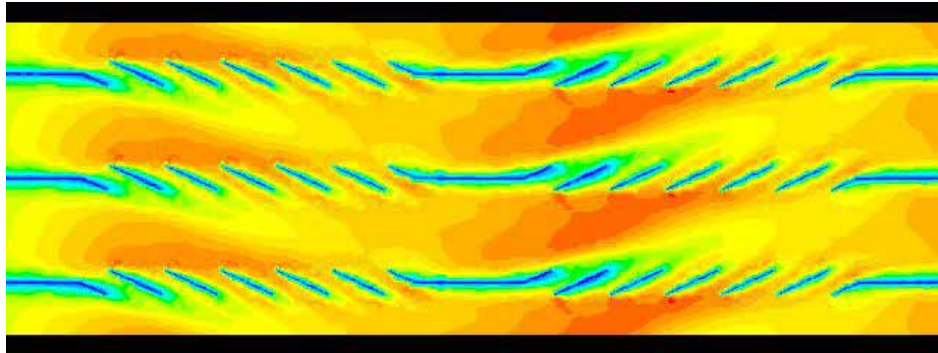
with variation in Θ implies that the main heat transfer mechanism is due to the influence of the leading edges, rather than any increase, or decrease in turbulence levels. We know from flow visualisation conducted by DeJong and Jacobi[78] that vortex shedding occurs more readily, as Θ increases, although they increased the louvre angle from 18 to 28 degrees. Referring to Figure 9.2.1 it is evident that for a louvre pitch of 2.08mm, which is the case most similar to our louvre pitch of 1.5mm, and considering Θ between 25° and 35°, there is very little variation in Nu Number. One can conclude that louver angle variation has very little affect on heat transfer performance unless the louver pitch is large or if there is a substantial increase in louvre angle from a relatively shallow angle².

Observation of the flow through the louvres helps to explain the results. Figure 9.4.1 is a plot of velocity contours along the first and second rows of louvres at the leading edge of the fin, and is typical of the flow through the louvres further downstream. It can be seen that in the case of $\Theta=25$ degrees, the first two louvres do not direct any of the flow and the low velocity and high pressure regions between these louvres create stagnation zones. Hence the bulk flow accelerates in the regions above the first two louvres. By the third louvre there is redirection of the flow in between the louvres and the bulk fluid experiences a reduction in velocity. Thus the effectiveness of the first two louvres with respect to heat transfer is compromised resulting in the lower heat transfer performance for the case of $\Theta=25^\circ$.

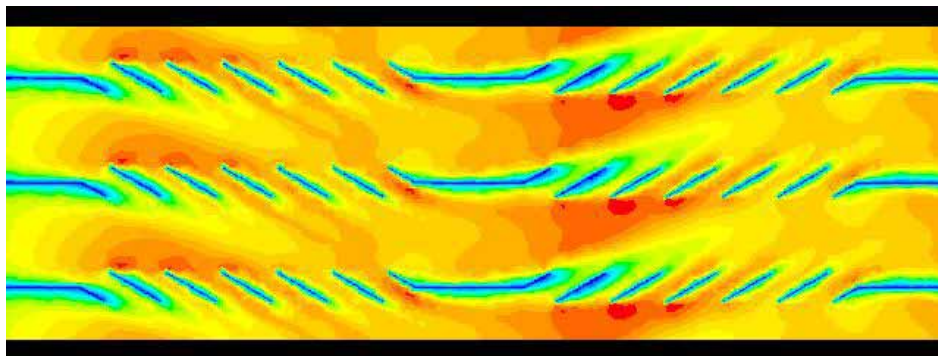
As the louvre possibly angle increases, the front louvres become more effective in directing the flow. When $\Theta=30$ degrees the second louvre is effective, and there is flow between the first and second louvres. For the case of $\Theta=35$ degrees the first louvre has some effect at redirecting the flow, and some weak flow can be seen between the landing and the first louvre. As the flow becomes more louvre directed, the bulk flow velocity is reduced. Because a greater proportion of the flow is directed through the louvres, their effectiveness improves and slightly higher heat transfer results.

² It should be pointed out that these results will vary at lower Reynolds Number flow since the flow will be less redirected, in part due to boundary layer blockage. Hence an increase in louvre angle would probably show a greater improvement. Simulations were not performed however as the primary motivation was to maximise performance at higher air speeds.

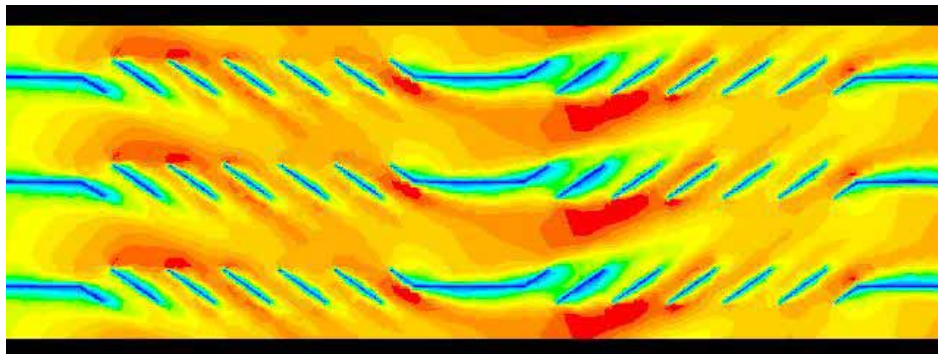
Hence it seems that the improved effectiveness of the louvres with increased Θ , is responsible for any improvement in heat transfer rather than any increase in turbulence.



a) $\Theta=25$ degrees



b) $\Theta=30$ degrees



c) $\Theta=35$ degrees



Legend: Air Velocity in m/s

Figure 9.4.1 Velocity contours through the first and second rows of louvres for varying louvre angle Θ . The air flow is from left to right.

The pressure drop is as a result of viscous drag along the louvre sides, and mechanical blockage due to the angle of incidence the louvres make with the approaching flow. The viscous contribution is dependant on the developing boundary layers on each of the louvre surfaces as well as the turning louvre. The boundary layer development is dependent on the local flow velocity which varies at each louvre position to a varying degree depending on the louvre angle, as mentioned previously.

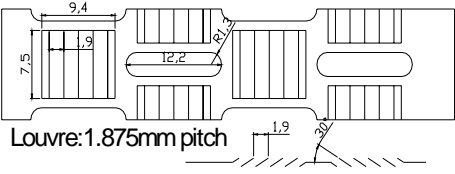
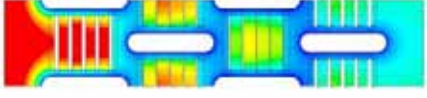
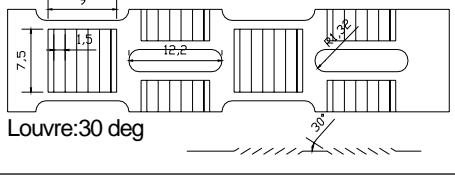

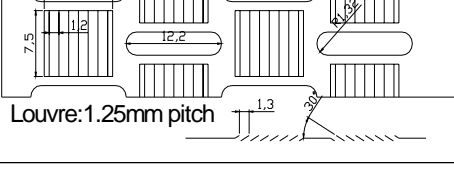

The main contribution to the pressure drop is due to the mechanical blockage as a result of the louvres projecting into the flow causing an increase in momentum as the flow is turned through an angle. For $\Theta=30^\circ$ the flow has to be turned through a greater angle to negotiate the second set of louvres, resulting in a higher pressure loss. In addition, the turning air flow approaches the second set of louvres at an increased angle of incidence resulting in more separation and larger wake zones behind the turning louvre and first louvres in the second louvre set. This possibly accounts for the higher pressure drop attributed to the increased louvre angle.

9.4.2 Louvre pitch variation

Table 9.2 summarises the performance results due to the variation of L_p for the three cases. As before, the values have been normalised with respect to the standard case of L_p equal to 1.5mm.

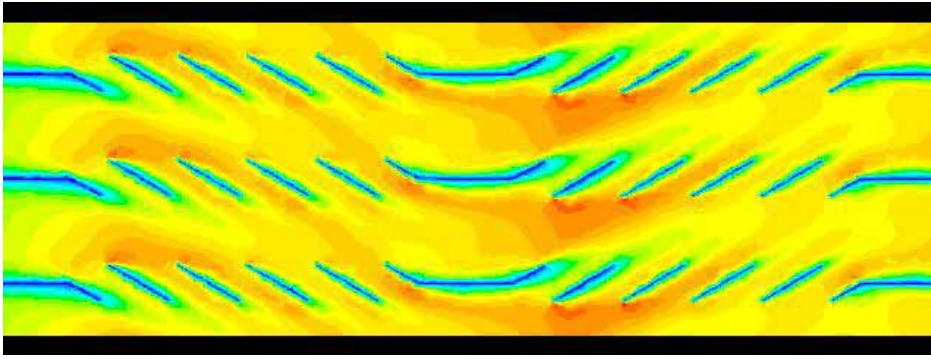
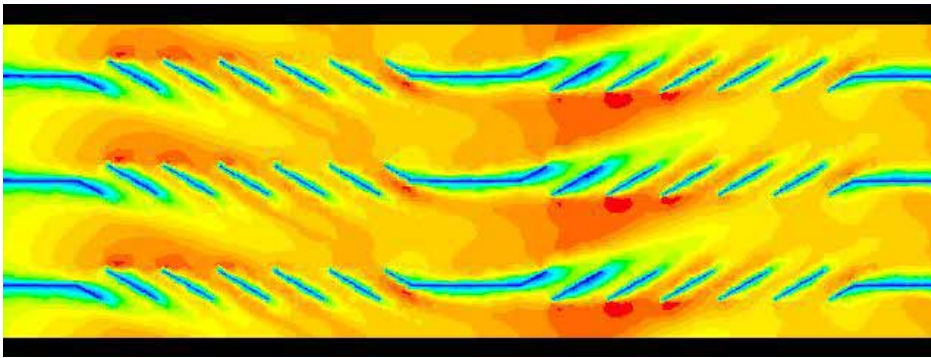
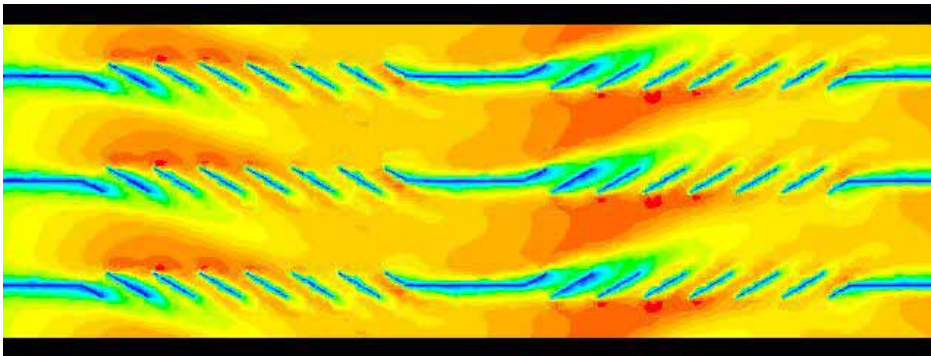
According to these results there is a 5% drop in heat transfer performance when the L_p is increased to 1.875mm, which also results in a decrease in louvre quantity for the same louvre area. When the L_p is reduced to 1.25mm resulting in an increase in the louvre quantity there is a 3% increase in heat transfer performance. Clearly the louvre quantity and hence leading edges has a measurable affect on heat transfer performance. These results support those found by Leu et al[51] as discussed in Section 9.2.

Table 9.2 Louvre fin performance comparison at 9 fpi with varying louvre pitch and constant louvre angle of 30 degrees

Louvre pitch (L_p)	Fin temperature contours	\dot{Q}	ΔP
 <p>Louvre: 1.875mm pitch</p>		0.95	0.99
 <p>Louvre: 30 deg</p>		1.00	1.00
 <p>Louvre: 1.25mm pitch</p>		1.03	1.00

The pressure drop in each case is similar, although a slight reduction in pressure drop was obtained with the larger L_p or fewer louvres. The viscous contribution would be expected to increase as the louvre quantity increases since the shear stresses on the leading edge of each louvre is large. The mechanical blockage contribution would be expected to decrease since the louvre height and projection into the bulk fluid zone is less. Therefore these two mechanisms compete with each other to result in the total pressure drop.

Figure 9.4.2 displays the resulting velocity contours occurring at the first and second sets of louvres for each case of variation in louvre pitch but having the same Θ .

a) $L_p = 1.875\text{mm}$ b) $L_p = 1.5\text{mm}$ c) $L_p = 1.25\text{mm}$ 

Legend: Air Velocity in m/s

Figure 9.4.2 Velocity contours through the first and second rows of louvres for varying louvre pitch. The air flow is from left to right.

It can be seen in the case of large L_p that the maximum velocity zones adjacent to the louvres in between fins is relatively lower. The louvres which project further into the

bulk flow are more effective at directing the flow. As the L_p is reduced the louvres are less effective at directing the flow resulting in higher velocities in between the fins. However the increase in leading edge quantity as L_p is reduced more than compensates for the reduction in louvre effectiveness, resulting in higher heat transfer performance.

In the case of low L_p , and hence 6 louvres, the viscous pressure drop dominates; conversely since the louvre height is correspondingly lower the mechanical blockage is lower. In the case of high L_p and hence 4 louvres, the viscous pressure drop is lower, but the projection of the louvre into the airstream is higher, effectively increasing the mechanical blockage. These two mechanisms oppose each other to varying degrees as the louvre pitch varies; ultimately resulting in a similar pressure drop in each case.

9.4.3 Louvres with serrated edges

Louvres are typically pressed from the fin surface by a combined cutting and rolling process using a circular cutter which mates with a corresponding rolling die. A serrated louvre would involve exactly the same manufacturing process, however instead of the cutters having straight edges; they would be wound round the rollers in a zig-zag. Figure 9.4.3 is a sketch of the meshed surface of the proposed serrated louvre geometry.

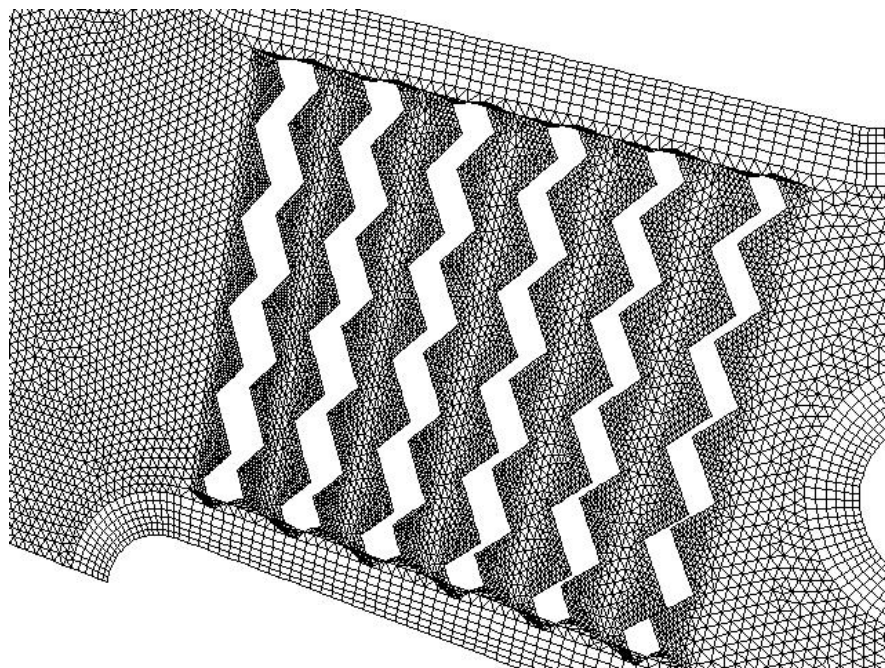
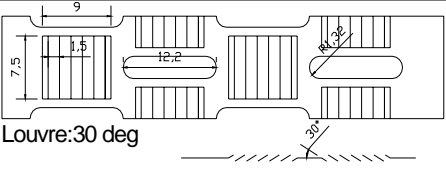
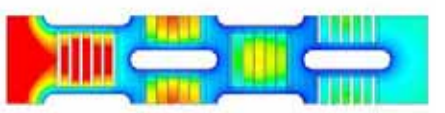
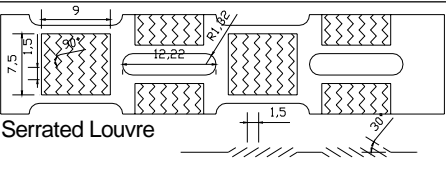
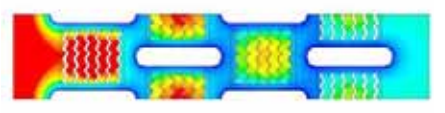


Figure 9.4.3 Sketch showing the meshed serrated louvre geometry

Table 9.3 compares the performance of the serrated louvre with the standard louvre surface, each having a pitch of 9fpi.

Table 9.3 Louvre fin performance comparison at 9fpi with serrated louvre at 9fpi

Serrated Louvre	Fin temperature contours	\dot{Q}	ΔP
 <p>Louvre: 30 deg</p>		1.00	1.00
 <p>Serrated Louvre</p>		0.99	0.99

The temperature contours of the two fin surfaces shown in Table 9.3 are remarkably similar. The same temperature distribution across the fin surface indicates similar heat transfer performance. Apparently serrating the louvre edges has no benefit over the straight edged louvres with respect to heat transfer performance. This is explained by considering that serrating the louvre edges does not actually increase the leading edge length. The serrated edges should be resolved into equivalent lengths that are normal to the flow in order to qualify as an apt leading edge. Therefore in spite of the serrations the effective length is in fact equal to the straight louvre edge. It is also apparent that the prospect of generating micro vortices along the louvre surfaces meets with little advantage. If vortices are indeed generated, it seems that they lack sufficient energy to enhance the convection there. It seems that turbulence or vortex generation at a leading edge which is already subject to boundary layer restarting is possibly a redundant measure which can not provide any additional convection enhancement.

9.4.4 Progressively varying Louvre angle

It was determined in chapter 7 that the largest proportion of heat transfer is undertaken by the front part of the fin, specifically from adjacent to the first tube row. Since the heat transfer in this region is already at a maximum, it is a challenging task

to enhance it further. This was reinforced by the results of chapter 8 which demonstrated that a leading edge vortex generator showed marginal overall heat transfer improvement in a louvre fin surface. It is thought that there is more potential in spreading some of the heat transfer towards the rear of the coil, where typically it is much lower. In order to test this proposal, a numerical model which featured a progressively increasing louvre angle towards the rear was trialled.

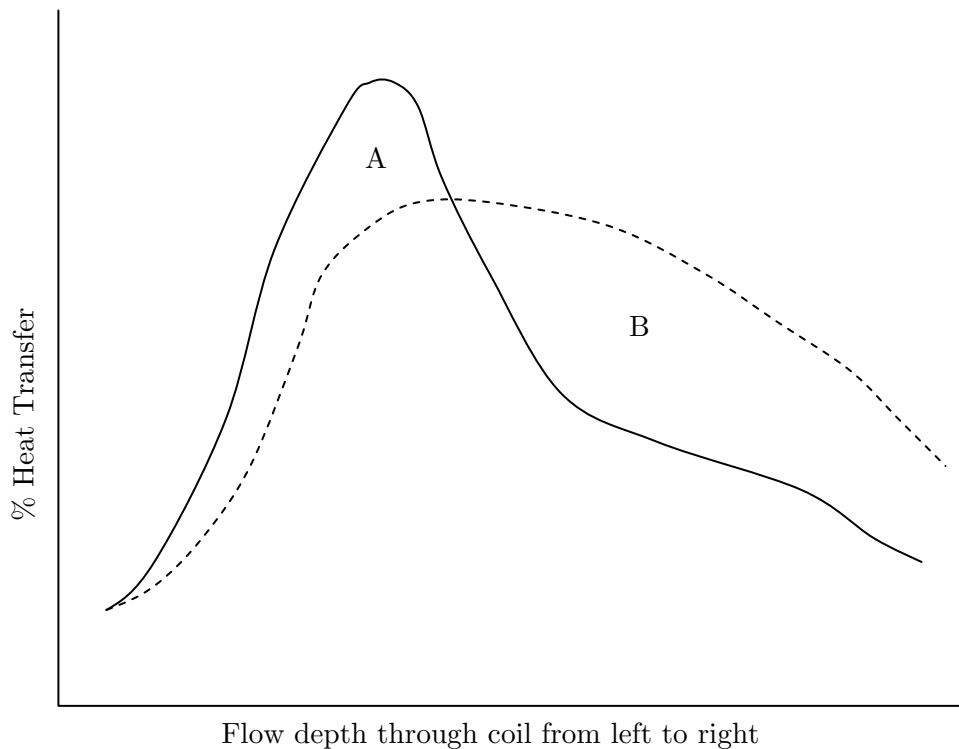


Figure 9.4.4 Sketch explaining the principle of shifting heat transfer performance to the rear of the coil. The coil has higher performance if Area B > Area A

The louvre angle was progressively increased in the x -direction from 15° at the first louvre row, then 25° , then 35° to 45° at the last louvre row. In addition the louvre direction was kept the same from row to row, contrary to typical fins where the louvre direction alternates for each successive row. The reason for this was that it was thought that this arrangement offered the best geometry for conveying undisturbed fluid from the front to the rear. The configuration of the louvres in the fin can be seen in Figure 9.4.5.

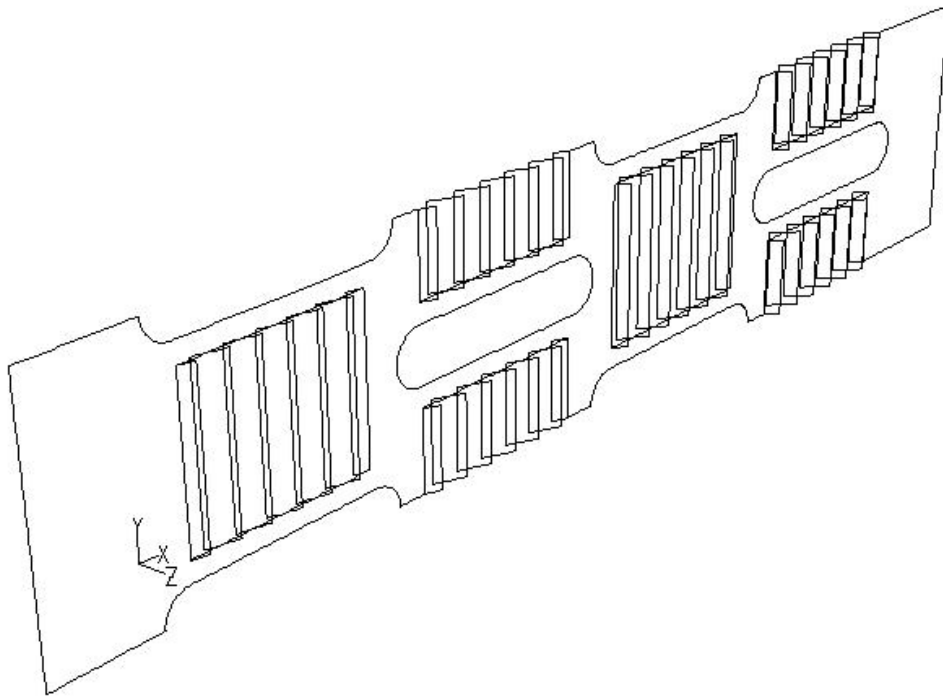


Figure 9.4.5 Sketch of the fin surface having progressively increasing louvre angle in the x -direction from 15° , then 25° then 35° and finally 45° at the last louvre row

Because the louvre direction was the same, additional options have been introduced with respect to the boundary conditions. If the adjacent fin is assumed to have louvres in the same direction as the model, then a periodic boundary condition should be selected. If it is assumed that the adjacent fin has louvres with an opposing direction then a symmetry boundary condition is warranted. This is further explained in Figure 9.4.6.

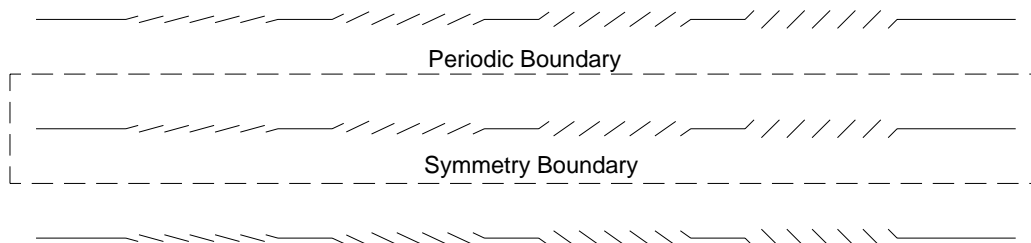
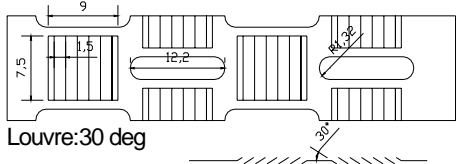
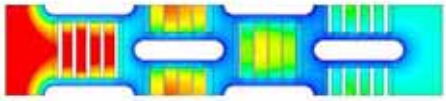
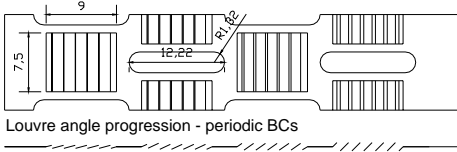
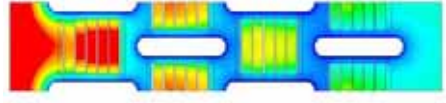
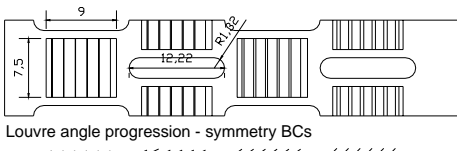
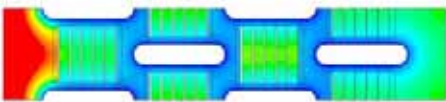
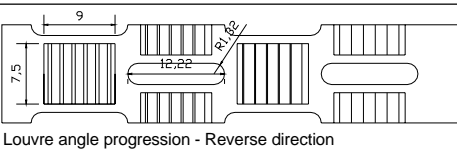
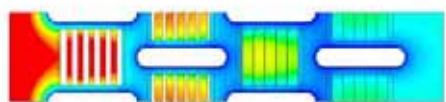
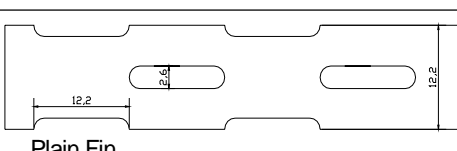



Figure 9.4.6 Sketch explaining the choice of suitable boundary conditions for each choice of fin assembly

For comparison, the model was simulated with both periodic and symmetry boundary conditions. In addition the results of a plain fin simulation are included. Finally, in order to truly test the proposed concept, it was decided to simulate the case of a reverse progression of louvre angle, where the louvre angle is progressively decreased from an initial angle of 45° at the front. The results of the Numerical simulation prediction of heat transfer and pressure drop are presented in Table 9.4.

Table 9.4 Louvre fin performance comparison at 9 fpi with progressively varying louvre angle

Louvre fin Surface	Fin temperature contours	\dot{Q}	ΔP
 <p>Louvre: 30 deg</p>		1.00	1.00
 <p>Louvre angle progression - periodic BCs</p>		1.01	1.13
 <p>Louvre angle progression - symmetry BCs</p>		0.86	1.49
 <p>Louvre angle progression - Reverse direction</p>		1.02	1.14
 <p>Plain Fin</p>		0.67	0.61

From Table 9.4 it is apparent that the case of the progressively varying louvre angle with periodic boundary conditions has slightly improved heat transfer performance than the standard louvre fin surface. However if the louvre angle progression is reversed the performance is slightly better. In both cases the pressure drop is higher by

approximately 13-14%. Irrespective of progressively increasing the louvre angle from inlet to outlet, or the reverse direction, there is minimal benefit in heat transfer improvement which is overshadowed by the higher increase in pressure drop.

Interestingly, for the case of progressively increasing louvre angle with symmetry boundary conditions the heat transfer performance is 0.86% of the standard louvre fin surface but has a 49% increase in pressure drop. Observing the fin temperature contours it is apparent that the whole of the fin surface including the louvres is at a lower temperature. This is undoubtedly due to the flow path being duct directed rather than louvre directed. The heat transfer progression through the coil in each case has been plotted in Figure 9.4.7.

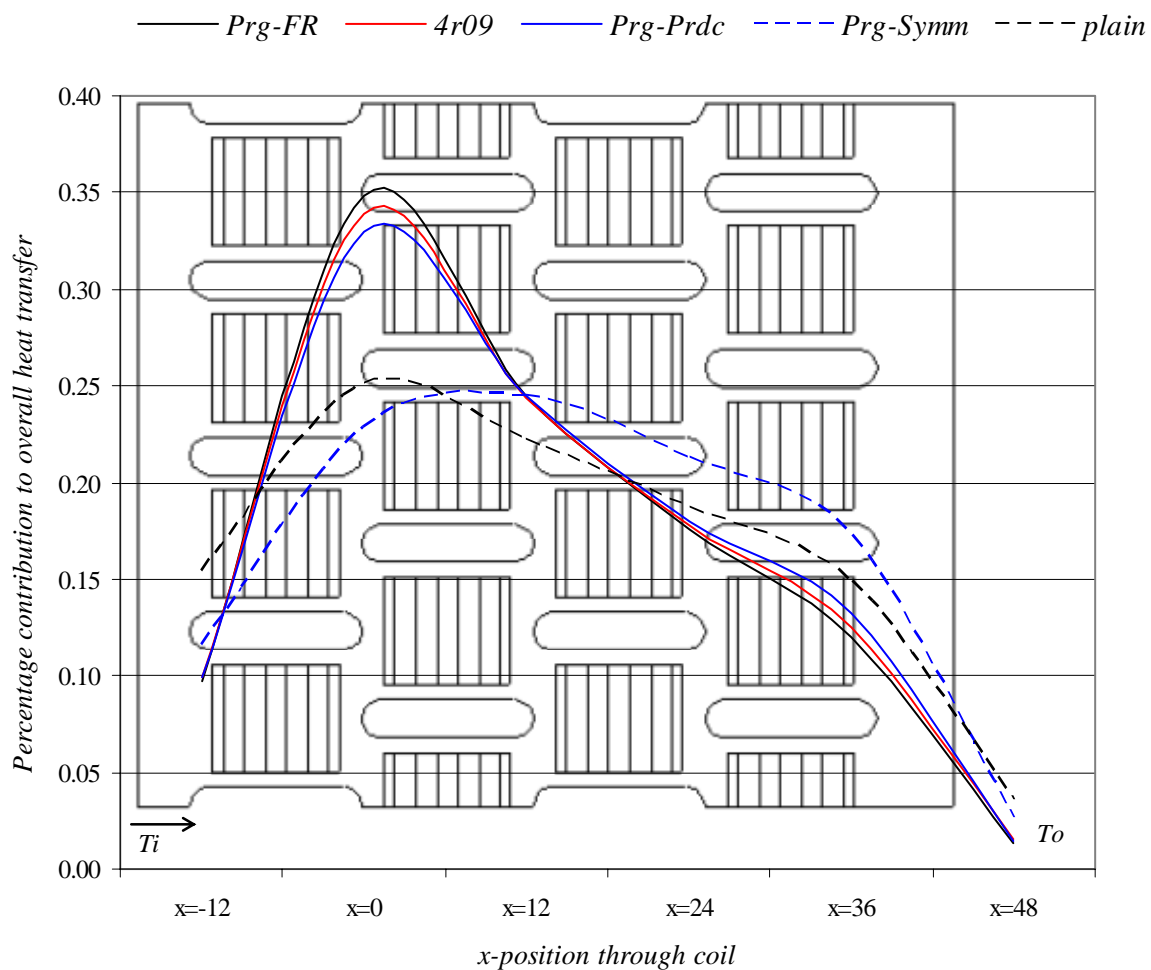


Figure 9.4.7 Graph plotting the % temperature change of the inlet air initially at T_i , at each x -position as it progresses through each coil

From Figure 9.4.7 it can be seen that for the case of the front louvres having the steepest angle, the heat transfer performance is slightly higher after the first tube row, and this results in the overall performance being higher. However there is a cross over point after the second tube row whereupon the heat transfer percentage of the coil with progressively increasing louvre angle is slightly greater towards the rear of the coil. This coil has a slightly lower temperature change after the first tube row than the standard louvre coil. But because there is a crossover point towards the rear there is a slight increase in heat transfer performance as predicted. In the case of the symmetry boundary conditions the percentage heat transfer contribution is similar to that of a plain fin resulting in the poor performance.

9.5 Concluding Remarks

The numerical investigation showed that increasing the louvre angle showed a slight increase in heat transfer performance but the increase in pressure drop was significantly greater. Also, increasing the louvre pitch, which decreases the number of leading edges, decreases the heat transfer performance. These findings are consistent with those of other researchers in the field as discussed in Section 9.2.

The numerical model having serrated louvre edges showed no heat transfer improvement. This is because there is no increase in the “effective” leading edge length. Also an observation of pathlines over the serrated edges showed no evidence of flow disturbance. This is because at the high inlet velocities and narrow fin pitch the flow is louvre directed. Therefore the flow is completely aligned with the louvre edges and hence minimal flow disturbance can occur.

Progressively increasing the louvre angle from inlet to exit, or visa versa, showed a slight increase in heat transfer performance above the standard louvre fin surface. However to achieve this, the fins have to be assembled along the tubes so that the louvres are aligned in the same direction. The slight improvement in heat transfer is accompanied by a larger increase in pressure drop.

Chapter 10

Conclusion

10.1 Homogeneous turbulence

A series of experiments with a heat exchanger coil constructed entirely of tubes forming a tube mesh heat exchanger (TMHE) was designed to exhibit homogeneous turbulence. The intention was to prevent flow laminarisation, and promote three dimensional turbulence, by having an open mesh design. The overall heat transfer capacity was considerably lower than standard parallel fins having louvred surfaces by about 50%. This was attributed to the small heat transfer area. It was demonstrated that the air side heat transfer coefficient h_o is significantly lower by about 20% than parallel fins having enhanced louvred surfaces. This can possibly be explained for two reasons. Firstly it is thought that the turbulence levels are not fully developed until some distance through the mesh which may compromise convection enhancement in the front tube rows. Secondly, homogeneous turbulence by definition may not be particularly effective as a convective medium, due to the homogeneity of the small scale eddies. One can infer that a more transport-specific flow structure such as a vortex may be more effective as a convective medium. Compared to the earlier study performed by Ko et al[59] which motivated this investigation, this coil does not have the capacity to generate specific vortices which are clearly more effective at enhancing convection. They were able to craft a surface which had specific sights of transverse vortex generation, namely at pin and fin junctions.

On the other hand, as a heat exchange device, the TMHE had an extremely low air pressure drop. This may prove useful for particular applications which require low air pressure drop.

10.2 Transverse Vortices combined with leading edges

The concept of parallel plate arrays combined with a tube array was studied in order to investigate the convection enhancement potential of transverse vortex shedding combined with leading edges in a tube and strut heat exchanger arrangement. A flow visualisation study showed that the resultant flow field through the exchanger is a combination of influences from the tubes and the displacement of fluid due to the finite thickness of the struts. The influence of the struts is highly dependent on the strut spacing. At the widest strut spacing, their influence is minimal, because the struts are located in relative isolation. In this case the flow structure behaves similar to that of a plain tube bank, and at higher Reynolds numbers von Kármán vortices are shed by the front rows of tubes. At the middle strut spacing the struts exert a combined influence on the bulk flow structure so that at a critical Reynolds number some transverse vortices are shed, which can be expected to improve heat transfer. However, as the Reynolds number is increased, the influence of the tube profile outweighs that of the struts and the flow resembles that of a plain tube bundle. At the narrowest strut spacing, the struts are so close together that they tend to suppress any transverse fluid motion and the flow remains laminar throughout.

The experimental results from testing actual coil prototypes corroborate the findings from the flow visualisation study. The prototype with the medium strut spacing had the highest capacity of the prototypes, and also demonstrated the highest levels of transverse vortex shedding during the flow visualisation studies. However its heat transfer capacity was about 65% of the louvre fin surfaces. This configuration, along with the other prototypes had considerably lower pressure drop than the louvre fin surfaces. These findings suggest that a strut thickness and strut spacing combination to achieve a heat transfer performance equivalent to the louvred fin surfaces is unlikely. The transverse vortices and quantity of leading edges is insufficient to make up for the lack of fin surface area. Increasing the number of struts to compensate for this is unachievable due to the space restriction caused by the thickness of the struts. However the thickness of the struts is seen to be an important geometrical requirement for the generation of vortices.

A numerical study was undertaken to examine the possibility of increasing the strut surface area by increasing the chord length rather than the quantity of struts. The study showed that to achieve the same performance of the louvre fin surfaces, a strut chord length of about 50mm would be required, which is almost the full depth of the coil, and therefore impractical.

Transverse vortices generated by parallel plate arrays do not provide sufficient convection enhancement, to compensate for the reduction in fin surface area. In addition there are insufficient leading edges compared to those in a louvred fin. Clearly some other turbulence generating devices in combination with the struts is required. However these would have to be carefully designed, to avoid causing additional flow interference.

10.3 Streamwise Vortices

Stream wise vortices are most conveniently generated by delta winglets. A prototype coil fin surface having flow-up delta winglet vortex generators was fabricated and its performance assessed, and compared with that of two standard louvre fin surfaces. The delta winglets were arranged in a hitherto untried flow-up configuration. The winglet pairs were placed directly in front of each tube (except for the first row, due to lack of space). Furthermore, the tubes of the coil were flat radiator tubes as opposed to circular tubes. Therefore this data has important experimental and commercial value. Flow visualisation experiments were performed to ensure that the winglet geometry created pronounced stream wise vortices.

The results were presented in the form of j -factor and f -factor plots alongside the two louvre fin surface results. The Reynolds number range, based on the tube diameter including collar thickness covered 650-1800, which is the useful range for this type of radiator application. It was found that at all Reynolds numbers, the heat transfer coefficient of the delta winglet surface was approximately 80% of that of the two louvre fin surfaces. On the other hand the fanning friction factor was about 50% of that of the louvre surfaces. Although the maximum capacity of the surface is lower, the very low pressure drop may make it suitable for particular applications. Or put another way, by increasing the coil size and hence air flow rate by 15% compared to a

similar louvre finned coil, the resulting coil would have the same capacity but less than half the pressure drop. This would result in a power consumption by the convection fan of 54% of that required by the louvre finned coil.

Alternatively it was demonstrated that by increasing the inlet air velocity by 30%, the delta-winglet coil would have comparable heat transfer capacity to the louvre fin coil having 9 *fpi*. This is achieved at a lower pressure drop of 89% of that of the louvre coil.

A numerical model was developed to represent these findings and was validated against the experimental results. The model was then used to simulate the heat transfer and pressure drop performance of many other delta winglet configurations. One aspect which hasn't been studied previously is the effect of leaning the delta alignment off the vertical. It was determined numerically that a lower pressure drop can be achieved with no loss in heat transfer performance, if the deltas are not completely vertical. Another range of simulations investigated the effect of doubling and tripling the number of winglets. Also the orientation was varied including combinations with flow-down delta winglets. In spite of trialling the most obvious combination of winglets, there were none that were able to match the capacity of the louvre fin surfaces. Also, an LES simulation showed that there are actually two vortices generated by the delta-winglet. Neither of the two vortices is suitably employed to provide substantial convection enhancement. This is mainly due to the fact that they are small in comparison with the fin geometry and suffer from diminished longevity.

These findings suggest that enhancement of a plain fin surface with any type of delta-winglet configuration is not as effective as an equivalent louvre fin surface. Increasing three dimensional vorticity, in order to improve the convection coefficient may have a localised benefit. However, in a tube and fin heat exchanger environment, unadulterated vortices can not be maintained throughout the array, especially if they are of a small scale. Interference from adjacent vortices and mechanical blockage from the downstream vortex generators does not provide for a vortex sustaining flow. In the confines between fins, the most effective heat transfer mechanism is by restarting of the boundary layer, rather than increasing turbulence. The most geometrically

appropriate way of increasing the number of leading edges can be found in a louvred fin arrangement.

10.4 Combined stream wise vortices with leading edges

A numerical study was performed to investigate the potential of using large scale vortices in combination with a louvred fin surface in order to increase heat transfer performance. Various delta profiles which were large in comparison to the louvre height were implemented on the fin leading edge at various incident angles. The fin pitch was increased to double that of the normal pitch, in order to accommodate the size of the delta.

It was found that in spite of the larger delta size the generated vortices were still not of a large enough scale to enhance the airside convection coefficient to compensate for the reduction in fin surface area. Due to the wide fin pitch, the louvre directed flow diverted the vortex from its stream wise path and forced it through the adjacent fin louvres where it was essentially dissipated. Hence only a minimal enhancement was realized. It can be inferred that at much lower Reynolds numbers where the flow is duct directed the vortex structure should have greater longevity due to the streamwise flow, and hence show a reasonable level of heat transfer enhancement above that of a plain louvre surface.

10.5 Leading edge enhancement

Louvre finned surfaces have the maximum geometrical capacity for increasing the number of leading edges. A numerical investigation was undertaken to investigate the effect of various geometrical parameters pertaining to louvre arrays. The variation in louvre angle, louvre pitch and a serrated louvre edge were assessed. In addition the prospect of shifting heat transfer towards the rear of the fin was investigated by introducing a progressively increasing louvre angle. Agreement was found with others that louvre angle has minimal effect on heat transfer performance. Similarly louvre pitch variation does not demonstrate significant heat transfer benefits.

A serrated louvre edge showed no actual heat transfer enhancement and likewise there was no increase in pressure drop. This is because the flow is aligned with the louvres in a louvre directed flow. Since the serrations do not project into the flow vortex generation can't be achieved. Similarly there is no increase in the effective leading edge length since only edges normal to the flow can be considered as leading edges.

It was found that by progressively varying the louvre angle a slight increase in heat transfer could be achieved. However this was accompanied by a larger increase in pressure drop.

10.6 Future work

It is believed that the tube mesh heat exchanger has the potential to suit particular applications, especially where a low pressure drop is a requirement. Of course the geometry would have to be optimised, primarily of course the tube spacing. Since homogeneous turbulence can not be expected to benefit the airside convection coefficient, more benefit may be derived by increasing tube surface area by reducing the tube spacing. Also vertical and horizontal tubes should be of equal length. This is important to ensure that high Reynolds numbers are achieved in both sets of tubes. The resulting square heat exchanger would obviate the need to balance the flow in the vertical and horizontal directions. A square heat exchanger is desirable since this makes it suitable for the mounting of an axial fan.

Similarly the tube strut heat exchangers may also be suited to particular applications. In order to reduce the coil weight while maintaining strut thickness, alternative strut materials could be used. We have learned that the conduction properties of the thick struts are unnecessary. Plastic or PVC struts may be tried. The existing range of CFD models could be easily adopted to perform this.

The delta-winglet fin surface has comparable heat transfer performance to a louvred fin surface but much lower pressure drop. This heat exchanger could have many useful applications. The range of applications however could be increased by a careful optimisation of the delta-winglet geometry. For example increasing the angle of incidence would certainly generate stronger vortices which would improve the enhancement. The extremely low pressure drop suggests that an increase in pressure

drop can be afforded. In addition, an experimental analysis of confirming the effect of having deltas which are not vertically aligned would be extremely beneficial.